The G-protein γ subunit DEP1 facilitates brassinosteroid signaling in rice via a MYB–bHLH–ARF module

Shuai Li[1,5], Zhichao Zhao[1,5], Tianzhen Liu[1,5], Jinhui Zhang[1,5], Xinxin Xing[1], Miao Feng[1], Xin Liu[1], Sheng Luo[1], Kun Dong[1], Jian Wang[1], Yupeng Wang[1], Feng Zhang[1], Rong Miao[2], Wenfan Luo[1], Cailin Lei[1], Yulong Ren[1], Shanshan Zhu[1], Xiuping Guo[1], Xin Wang[1], Qibing Lin[1,*], Zhijun Cheng[1,4,*] and Jianmin Wan[1,2,3,*]

[1]State Key Laboratory of Crop Gene Resources and Breeding, Institute of Crop Sciences, Chinese Academy of Agricultural Sciences, Beijing, 100081, China
[2]State Key Laboratory for Crop Genetics and Germplasm Enhancement, Nanjing Agricultural University, Nanjing, 210095, China
[3]Zhongshan Biological Breeding Laboratory, Nanjing, 210014, China
[4]Nanfan Research Institute, Chinese Academy of Agricultural Sciences, Sanya, 572025 China
[5]These authors contributed equally to this article.
***Corresponding authors**: **Qibing Lin** (linqibing@caas.cn),
Zhijun Cheng (chengzhijun@caas.cn),
Jianmin Wan (wanjianmin@caas.cn)

Short title: G-protein-derived pathway activates BR responses

Key words: G-protein; BR signaling; Leaf inclination.

The author responsible for distribution of materials integral to the findings presented in this article in accordance with the policy described in the Instructions for Authors (https://academic.oup.com/plcell/pages/General-Instructions) is Jianmin Wan (wanjianmin@caas.cn).

Abstract

G-protein signaling and brassinosteroid (BR) phytohormones play important roles in regulating rice (*Oryza sativa*) yield-related plant architecture, such as leaf inclination and grain size. However, the relationship between G-proteins and BR signaling has not been fully elucidated in rice. The present study indicates that the G-protein Gγ subunit DENSE AND ERECT PANICLE 1 (DEP1) positively regulates BR signaling in rice and that BRs promote DEP1 nuclear entry through GRAIN NUMBER ASSOCIATED (GNA). Additionally, DEP1 interacts with and acts upstream of OsMYB86, an R2R3-MYB family transcription factor that positively regulates BR signaling by

directly binding to the promoter of its downstream gene *BRASSINOSTEROID UPREGULATED 1* (*BU1*), activating its expression in rice. In the nucleus, DEP1 interacts with OsMYB86 and GNA, significantly enhancing OsMYB86-mediated activation of *BU1* expression. Furthermore, BU1 interacts with another HLH protein, INCREASED LEAF INCLINATION1 (ILI1), and a bHLH protein, ILI1 BINDING bHLH (IBH1). Interaction between ILI1 and BU1 facilitates translocation of BU1 from the cytoplasm to the nucleus, where they impede IBH1 binding to the promoter of the *AUXIN RESPONSE FACTOR 11* (*OsARF11*) gene, which is involved in crosstalk between BR and auxin, thus effectively relieving the IBH1-repressed transcription of *OsARF11*. These findings reveal a DEP1-mediated signaling pathway that links G-proteins to the traditional BR signaling pathway, ensuring the efficient activation of BR responses in rice.

Introduction

Leaf inclination, the inclination between the leaf blade and the culm, is an important character affecting rice plant architecture (Zhou et al., 2017). In rice plants erect leaves can enhance photosynthetic efficiency, nitrogen storage, and planting density, thus they have great potential for improving rice productivity (Sakamoto et al., 2006). Leaf inclination is mainly controlled by lamina joint development (Zhou et al., 2017), which is influenced by several factors including plant hormones (Sun et al., 2015), soil phosphorus content (Ruan et al., 2018; Guo et al., 2022), mechanical tissues (Ning et al., 2011; Huang et al., 2021), and gravitropism (Morita and Tasaka, 2004).

Stimulating lamina joint development is a typical effect of brassinosteroids (BRs), a class of steroid hormones found in plants (Tanabe et al., 2005; Sakamoto et al., 2006; Sun et al., 2015). There is growing evidence that many other phytohormones, including auxin (Qiao et al., 2022), gibberellin (Shimada et al., 2006), and abscisic acid (Li et al., 2019; Li et al., 2021) act synergistically or antagonistically with BRs to influence leaf inclination in rice. BRs are also involved in various plant growth and development processes such as cell expansion and division, floral organogenesis, leaf growth, grain development, and resistance to biotic and abiotic stresses (Bishop and Koncz, 2002; Nakashita et al., 2003; Tong et al., 2012; Tong and Chu, 2018; Nolan et al., 2020). Patterns of BR signaling and biosynthesis pathways in plants have been gradually revealed over the last few decades (Zhao and Li, 2012; Kim and Russinova, 2020).

Several crucial enzymes that biosynthesize BRs can affect BR levels in plants, leading to changes in leaf inclination. The *BRASSINOSTEROID-DEFICIENT DWARF2* (*BRD2*) gene encodes a protein with FAD-linked oxidoreductase activity, and a mutant form resulted in a typical BR-deficient phenotype with erect leaves (Hong et al., 2005). *Ebisu Dwarf* (*D2*), *Brassinosteroid-deficient dwarf1* (*BRD1*), *Dwarf11* (*D11*), and *Dwarf4* encode members of the cytochrome P450 family, and loss of their functions inhibits BR biosynthesis, resulting in smaller leaf inclination (Mori et al., 2002; Hong et al., 2003; Tanabe et al., 2005; Sakamoto et al., 2006).

In *Arabidopsis thaliana* BRs interact with the receptor BRASSINOSTEROID-INSENSITIVE 1 (BRI1) (Hothorn et al., 2011) and its coreceptor BRI1-ASSOCIATED RECEPTOR KINASE 1 (BAK1) (Li et al., 2002). The binding of BRs to BRI1 induces BRI1 KINASE INHIBITOR 1 (BKI1) disassociation and transphosphorylation between BRI1 and its coreceptor BAKs, leading to phosphorylated BSK release from BRI1 (Wang and Chory, 2006). Phosphorylated BSK proteins catalyze the phosphorylation and activation of BRI1-SUPPRESSOR 1 (BSU1) (Tang et al., 2008; Kim et al., 2011). Activated BSU1 dephosphorylates and inactivates Brassinosteroid-Insensitive 2 (BIN2), which functions as a repressor of BR signaling and inhibits BR responses by phosphorylating Brassinazole-Resistant 1/2 (BZR1/2), resulting in their transport out of the cytoplasm with the help of 14-3-3 protein (Li and Nam, 2002; Bai et al., 2007; Gampala et al., 2007; Clouse, 2011). Loss of BIN2 activity leads to dephosphorylation of BZR1/2. Lastly, dephosphorylated BZR1/2 accumulates in the nucleus, and regulates the expression of BR-responsive genes (He et al., 2005; Sun et al., 2010).

In rice, *OsBRI1* and *OsBAK1* function as BR receptors and coreceptors, and loss-of-function *OsBRI1* and *OsBAK1* mutants exhibit an erect leaf phenotype (Yamamuro et al., 2000; Park et al., 2011). Knockdown of GLYCOGEN SYNTHASE KINASE3 (GSK3)/SHAGGY-like kinase (*GSK2*), a rice homolog of *BIN2*, enhances OsBZR1 transcriptional activity and leaf inclination (Qiao et al., 2017). Several transcription factors including GROWTH-REGULATING FACTOR4 (GRF4) (Che et al., 2015; Duan et al., 2015), SMALL ORGAN SIZE1 (SMOS1) /REDUCED

LEAF ANGLE1 (RLA1) (Qiao et al., 2017), DWARF AND LOW-TILLERING (DLT) (Tong et al., 2012) and OVATE FAMILY PROTEIN1 (OFP1) (Xiao et al., 2017) function downstream of GSK2 and positively regulate leaf inclination in rice. *TAIHU DWARF1* (*TUD1*) encodes a U-box family E3 ubiquitin ligase that promotes BR signaling by interacting with the G-protein alpha subunit RGA1 and GSK2 (Hu et al., 2013; Liu et al., 2023). *GNA/DLT2/OsGRAS19* encodes a GRAS-type transcription factor and participates in BR signaling by interacting with DLT and BZR1 (Chen et al., 2013; Zou et al., 2023; Zhang et al., 2024). Downstream of OsBZR1, the basic helix-loop-helix (bHLH) transcription factors ILI1 and IBH1 act antagonistically to regulate rice leaf inclination (Zhang et al., 2009a). LIC and BZR1 antagonistically regulate the expression of *ILI1* and *IBH1*(Zhang et al., 2012). *BU1* encodes an HLH transcription factor lacking DNA-binding ability, and has been proposed to positively regulate BR signaling (Tanaka et al., 2009). There are many MYB genes in rice, and they also participate in BR signaling (Yanhui et al., 2006; Feller et al., 2011). For example, REGULATOR OF LEAF INCLINATION 1 (RLI1) and OsGAMYBL2 regulate leaf inclination in rice by regulating the expression of *BU1* and *BU1-LIKE1 COMPLEX1* (Gao et al., 2018; Ruan et al., 2018). Although *BU1*, *ILI1*, *IBH1*, and some MYB family genes reportedly regulate leaf inclination and BR signaling in rice, their specific functions have not been fully elucidated. Further studies are needed to clarify their specific roles.

G-proteins, composed of Gα, Gβ, and Gγ subunits, serve as signal transduction hubs in both plant and animal cells (Urano et al., 2013; Urano and Jones, 2014). The G-protein alpha subunit RGA1 has been implicated in both BR and GA signaling pathways in rice (Ueguchi-Tanaka et al., 2000; Wang et al., 2006). The Gβ subunit RGB1 promotes ABA biosynthesis, and the Gγ subunit DEP1 represses ABA responses (Zhang et al., 2015a). DEP1 interacts with Gα subunit RGA1 and Gβ subunit RGB1, and reduced RGA1 activity or increased RGB1 activity leads to nitrogen response inhibition (Sun et al., 2014; Sun et al., 2018). Rice varieties with dominant *dep1* mutation exhibit typical erect leaves (Huang et al., 2009; Sun et al., 2018). *DEP1*-overexpressing plants also exhibit a notably increased leaf inclination phenotype (Sun et al., 2018). DEP1 cooperatively

activates the expression of *REGULATOR OF LEAF ANGLE* (*OsRELA*)/*DENSE AND ERECT PANICLE 2* (*DEP2*) by interacting with BR signaling pathway transcription factor SMOS1/RLA1/GRAIN ROUND 5 (GR5) (Qiao et al., 2017; Wang et al., 2024). OsRELA/DEP2 interacts with the BR signaling negative regulator LEAF AND TILLER ANGLE INCREASED CONTROLLER (OsLIC), inhibiting its transcriptional activity, thus promoting leaf inclination in rice (Zhu et al., 2021). These findings suggest that *DEP1* likely plays a role in the BR signaling pathway, but the detailed pathway by which DEP1 regulates BR signaling remains unclear.

Here, we found that through GNA, BRs promote DEP1's entry into the nucleus, where DEP1 interacts with OsMYB86, activating OsMYB86-mediated transcription of *BU1*. Further, ILI1 interacts with BU1 and promotes the translocation of BU1 from the cytoplasm to the nucleus, where together they alleviate IBH1-repressed transcription of *OsARF11*, thus promoting BR signaling. Thus, these findings reveal a DEP1-GNA-OsMYB86- BU1/ILI1/IBH1-*OsARF11* signaling pathway that intricately connects the G-protein subunit DEP1 with the BR signaling pathway in rice.

Results

DEP1 is a positive regulator of BR signaling

To investigate the role of DEP1 in BR signaling, we created *DEP1* knockout (*dep1-1/2*) and *DEP1* overexpressing (*DEP1-OE*) lines, in the rice variety Kitaake (**Supplementary Figure S1**). The *dep1-1/2* plants showed erect flag leaves with reduced lamina inclination, while the *DEP1-OE* plants displayed flag leaves with increased lamina inclination compared to wild type (WT) plants (**Fig. 1A**, **1B**). Consistent with previous reports (Sun et al., 2018; Wang et al., 2024), *dep1-1* and *dep1-2* plants had smaller grain length, whereas *DEP1-OE* plants had larger grain length (**Fig. 1C**, **1D**). In lamina inclination assays, *dep1-1* and *dep1-2* plants exhibited reduced sensitivity to 2,4-epibrassinolide (2,4-epiBL) treatment compared to WT, whereas *DEP1-OE* plants exhibited enhanced sensitivity (**Fig. 1E**, **1F**). In coleoptile elongation assays *dep1-1* was also less sensitive

to 2,4-epiBL treatment than WT (**Supplementary Figure S2**). In RNA-Seq experiments, Gene Ontology (GO) enrichment analysis revealed that the DEGs between *dep1-1* and WT were enriched for annotated biological functions associated with hormone response, hormone-mediated signaling pathways, and hormone metabolic processes (**Supplementary Figure S3**). A heatmap showed that, compared to WT, the expression levels of several genes involved in BR signaling and biosynthesis were altered in *dep1-1* and *DEP1-OE* transgenic plants (**Supplementary Figure S4**). Expression of *OsHLH92* (Teng et al., 2023), *OsOFP22* (Chen et al., 2021), and *ILI1* (Zhang et al., 2009a), three BR positive response genes, was significantly increased by 2,4-epiBL treatment in WT, but it was suppressed in *dep1-1* mutants (**Supplementary Figure S5A-5C**). Expression levels of *IBH1* (Zhang et al., 2009a), *OsGRF4* (Duan et al., 2015), and *DLT* (Tong et al., 2009)—three BR negative response genes—were downregulated by 2,4-epiBL treatment in WT plants, but these responses were also disrupted in *dep1-1* mutants (**Supplementary Figure S5D-5F**). Expression levels of *D2*, *D11*, and *BRD2* were downregulated by 2,4-epiBL treatment in WT, but they were upregulated in *dep1-1* mutants (**Supplementary Figure S5G-5J**). This is consistent with previous reports that expression of some BR synthesis genes was downregulated by BL due to BR feedback inhibition (Tong et al., 2009; Qiao et al., 2017), and suggests that loss of *DEP1* function likely interferes with the normal BR feedback inhibition pathway. Substantial upregulation of *DEP1* expression was observed after 1 hour of treatment with 1 μM 2,4-epiBL (**Fig. 1G**), indicating that DEP1 plays a positive role in regulating flag leaf inclination in rice by responding to BRs.

BRs promote DEP1 nuclear entry through GNA

Many previous studies have identified different subcellular DEP1 localization patterns (Huang et al., 2009; Zhou et al., 2009; Taguchi-Shiobara et al., 2011; Sun et al., 2014; Liu et al., 2018; Matsuta et al., 2018; Sun et al., 2018; Miao Liu et al., 2021; Wang et al., 2024). Some previous studies have shown that DEP1 can be localized in the nucleus (or translocated) into the nucleus to interact with a number of transcription factors (Liu et al., 2018; Miao Liu et al., 2021; Wang et al.,

2024). Our recent findings revealed that GNA can effectively facilitate the nucleus entry of DEP1 (Zhang et al., 2024). Additionally, previous research has demonstrated that BRs promote the accumulation of GNA proteins in both *Nicotiana benthamiana* and rice (Chen et al., 2013; Zou et al., 2023). To explore the detailed mechanism by which BRs regulate the subcellular localization of DEP1, we analyzed its localization in rice protoplasts and *N. benthamiana* leaves. Three DEP1-GFP localization types were observed in Nipponbare protoplasts, with different percentages; type I, cytoplasmic and membrane localization without nuclear localization signals of DEP1-GFP (41%), type II, cytoplasmic and membrane localization with nuclear membrane outline (43%), and type III, cells with evident nuclear localization (16%) (**Fig. 2A, 2D**). Only two localization types, type I (50%) and type II (50%), were observed in protoplasts of the BR synthesis-deficient mutant *brd1*, and DEP1-GFP did not show clear nuclear localization in *brd1* protoplasts (**Fig. 2B, 2D**). However, co-expression of DEP1-GFP with GNA-FLAG in *brd1* protoplasts restored the nuclear localization of DEP1-GFP (**Fig. 2C, 2D**). Western blot analysis further validated these observations (**Fig. 2E**). After transforming the leaf epidermal cells of *N. benthamiana* with Agrobacterium for 60 to 72 hours, DEP1-GFPs are localized in the membrane and cytoplasm, with only approximately 4% cells exhibiting an evident nuclear membrane outline (**Supplementary Figure S6A**). Co-expression of DEP1-GFP and GNA-FLAG resulted in nuclear localization of DEP1-GFP in approximately 14% cells (**Supplementary Figure S6B, 6E**). BL treatment resulted in relatively weak nuclear localization of DEP1-GFP in approximately 20% cells (**Supplementary Figure S6C, 6E**). Following BL treatment, approximately 35% of leaf epidermal cells co-expressing DEP1-GFP and GNA-FLAG exhibited the most prominent nuclear localization signals of DEP1-GFP. (**Supplementary Figure S6D, 6E**). Western blot analysis further confirmed that the combination of BL and GNA-FLAG exhibited the highest efficiency in promoting DEP1 nuclear localization in *Nicotiana benthamiana*. (**Supplementary Figure S6F**). Based on these findings, we conclude that BRs facilitate DEP1 nuclear entry via GNA.

DEP1 interacts with OsMYB86

To delve deeper into the molecular mechanism of DEP1 involvement in BR signaling, we conducted a yeast two-hybrid screening and identified a candidate protein, OsMYB86 (**Fig. 3A, Supplementary Figure S7**). OsMYB86 is a typical transcription factor of the R2R3-MYB family which is widely expressed in different tissues, with high expression levels in the panicles of rice (**Supplementary Figure S8-10**). Interaction between DEP1 and OsMYB86 was further verified by a bimolecular fluorescence complementation (BiFC) assay (**Fig. 3B**), a luciferase complementation imaging (LCI) assay (**Fig. 3C**), and a co-immunoprecipitation (Co-IP) assay in *N. benthamiana* leaves (**Fig. 3D**). As well as DEP1, OsMYB86 also interacted with two other Gγ subunits, GS3 and GGC2, but did not interact with the Gα subunit (RGA1), the Gβ subunit (RGB1), or GNA (**Fig. 3A, Supplementary Figure S11**). Co-expression of DEP1-GFP with OsMYB86-FLAG in *N. benthamiana* leaves led to nuclear localization of DEP1-GFP in approximately 4% of the cells (**Supplementary Figure S12**). In comparison with protoplasts derived from WT Kitaake, the percentage of type III cells expressing DEP1-GFP in the *osmyb86* mutant protoplasts diminished from 11% to 4% (**Supplementary Figure S13**). These results indicate that OsMYB86 can interact with DEP1, but its capacity to facilitate the nuclear translocation of DEP1 is significantly weaker than that of GNA.

OsMYB86 positively regulates BR signaling by directly activating *BU1* expression

To investigate whether *OsMYB86* is related to BR signaling, knockout lines (*osmyb86-1,2,3*) and overexpressing lines (*OsMYB86-OE-1,2,3*) of Kitaake were generated (**Supplementary Figure S14**). Compared to WT, flag leaf inclination and grain length were reduced in *osmyb86-1,2,3* plants, whereas they were increased in *OsMYB86-OE* plants (**Fig. 4A–4D**). *Osmyb86-1,2,3* plants exhibited no significant changes in grain width or grain thickness. One *OsMYB86-OE* line exhibited increased grain width, and two *OsMYB86-OE* lines exhibited increased grain thickness (**Supplementary Figure S15**). Compared to WT, *osmyb86-1* and *osmyb86-3* plants were

hyposensitive to 2,4-epiBL, whereas *OsMYB86-OE-1* and *OsMYB86-OE-2* plants were hypersensitive to 2,4-epiBL (**Fig. 4E**, **4F**). *OsMYB86* expression was induced after 1 hour of treatment with 1 μM 2,4-epiBL, and 12 hours of treatment with 1 μM 2,4-epiBL (**Fig. 4G**). These results indicate that *OsMYB86* positively regulates BR signaling, controlling flag leaf inclination in rice.

To identify OsMYB86's direct downstream targets, chromatin immunoprecipitation-sequencing (ChIP-seq) analysis was performed using *OsMYB86-GFP* plants (**Supplementary Figure S16**). Two biological ChIP-seq repeats were conducted, resulting in coenrichment of 1028 genes associated with the binding site. Among these, we found that three putative OsMYB86 target genes, *BZR1*, *BU1*, and *GRF4*, were related to the BR signaling pathway (**Fig. 5A, Supplementary Figure S17**). To confirm this finding, expression levels of *BZR1*, *BU1*, and *GRF4* were analyzed in WT plants, and *OsMYB86-OE* and *osmyb86-3* mutant plants. *BU1* exhibited higher expression in the lamina joint of *OsMYB86-OE* plants, but lower expression in that of *osmyb86-3* mutant plants, compared to WT (**Fig. 5B, Supplementary Figure S17**). *BU1* expression was induced efficiently by 2,4-epiBL in WT seedlings, and more efficiently in *OsMYB86-OE* seedlings, but not in *osmyb86-3* mutant seedlings (**Fig. 5C**), suggesting that *BU1* may be the direct target gene regulated by OsMYB86. ChIP-qPCR experiments were performed to test this hypothesis, and substantial enrichment of the P1 and P2 segments of the *BU1* promoter sequence by OsMYB86 was evident (**Fig. 5D** and **5E**). Notably, both segments contain the core binding sequence [C/T]NGTT[G/T] recognized by R2R3-MYB family proteins (Millard et al., 2019). An electrophoretic mobility shift assay (EMSA) confirmed that OsMYB86-MBP binds directly to segment P1 of the *BU1* promoter (**Fig. 5F**). Consistent with a previous report (Tanaka et al., 2009), the *BU1* loss-of-function mutant exhibited an erect leaf phenotype, whereas *BU1*-overexpressing plants had increased leaf inclination compared to WT (**Fig. 5G–5J, Supplementary Figure S18**). As expected, the erect leaf phenotype of *osmyb86-3* mutant plants was substantially suppressed by *BU1* overexpression (**Fig. 5G**, **5H**), and the enlarged leaf inclination phenotype of *OsMYB86-OE*

plants was substantially suppressed by loss of *BU1* function (**Fig. 5I**, **5J**). Collectively these results indicate that OsMYB86 likely functions upstream of *BU1* in the BR signaling pathway by directly binding to the *BU1* promoter, activating its expression.

DEP1 acts upstream of OsMYB86 to boost OsMYB86-activated expression of *BU1*

Both DEP1 and OsMYB86 are positive regulators of BR signaling, and they exhibit physical interaction. To investigate the genetic relationship between them a *DEP1-OE/osmyb86-3* hybrid was generated by crossing *DEP1-OE* and *osmyb86-3* plants, and a *dep1-1/OsMYB86-OE* hybrid was generated by crossing *dep1-1* and *OsMYB86-OE* plants. The flag leaf inclination of *DEP1-OE/osmyb86-3* plants was closer to *osmyb86-3* plants compared to *DEP1-OE* plants (**Fig. 6A, 6B**), indicating that *DEP1*'s role in regulating rice leaf inclination is dependent on *OsMYB86*. In contrast, the flag leaf inclination of *dep1-1/OsMYB86-OE* plants were closer to that of *OsMYB86-OE* plants compared to *dep1-1* plants (**Fig. 6C, 6D**), suggesting that *OsMYB86* overexpression can complement the reduced leaf inclination phenotype caused by loss of *DEP1* function. These genetic results demonstrate that *OsMYB86* functions downstream of *DEP1* in the regulation of rice flag leaf inclination.

As mentioned above, OsMYB86 positively regulates BR signaling by directly activating *BU1* expression. RNA-seq analysis revealed that *dep1*, *bu1*, and *gna* share a number of differentially expressed genes (DEGs) (**Supplementary Figure S19A**), and most of the shared DEGs in *dep1*, *bu1*, and *gna* were changed in the same manner (**Supplementary Figure S19B-19D**), suggesting that *DEP1*, *GNA*, and *BU1* may share a common transcriptional module to regulate rice leaf inclination. In quantitative transactivation assays, co-transfection of ProBU1:LUC & Pro35S:DEP1-FLAG or ProBU1:LUC & Pro35S:DLT2-FLAG did not increase LUC activity. Co-transfection of ProBU1:LUC & Pro35S:OsMYB86-GFP & Pro35S:DEP1-FLAG resulted in a higher LUC activity compared to co-transfection with ProBU1:LUC & Pro35S:OsMYB86-GFP (**Fig. 6E and 6F**). These results suggest that DEP1 enhances the transcriptional activation of *BU1*

by OsMYB86. Co-transfection of ProBU1:LUC & Pro35S:OsMYB86-GFP & Pro35S:DEP1-FLAG & Pro35S:GNA-FLAG, followed by BL treatment, resulted in the highest LUC activity (**Fig. 6E and 6F**), which is consistent with the strongest nuclear localization signals of DEP1 conferred by BL and GNA (**Supplementary Figure S6D-6F**), suggesting that enhanced nuclear entry of DEP1 promotes the transcription of *BU1*. Supporting this, in RT-qPCR analysis *BU1* expression was reduced in *dep1-1* and *gna* mutants compared to WT plants (**Fig. 6G and 6H**). Similar to *osmyb86-3* mutants, BL-induced upregulation of *BU1* expression was also substantially suppressed in *dep1-1* mutants (**Fig. 6I**). In EMSAs, MBP-OsMYB86 but not MBP-DEP1 or GST-GNA fusion proteins were able to directly bind to *BU1*-probe. Moreover, DEP1 or GNA did not enhance the binding ability of OsMYB86 to the *BU1* promoter (**Fig. 6J**). Taken together, these results suggest that DEP1 augments the OsMYB86-mediated transcriptional activation of *BU1* with the help of GNA, likely by facilitating OsMYB86's function, rather than by increasing its binding affinity to the *BU1* promoter.

Mutants with loss of Gα (RGA1) function are insensitive to BL (Wang et al., 2006). DEP1 interacts with RGA1, and its role in regulating grain size is dependent on it (Sun et al., 2018). *BU1* is a primary BR signaling response gene that functions via both OsBRI1 and RGA1 (Tanaka et al., 2009). Interestingly, the enlarged leaf inclination phenotype of the *OsMYB86-OE* line was significantly suppressed by the loss of *RGA1* function (**Supplementary Figure S20**). These findings indicate that the function of OsMYB86 in the BR signaling pathway is also dependent on RGA1, the crucial G-protein signaling switch.

BU1 interacts with and functions upstream of IBH1 and ILI1

BU1 is a putative non-DNA-binding HLH protein, thus it may function by interacting with other bHLH proteins (Tanaka et al., 2009). To test this hypothesis a yeast two-hybrid assay was performed using pGBKT7-BU1 and proteins of the bHLH family known to be involved in BR signaling in rice. BU1 interacted with ILI1 or IBH1 in yeast cells (**Fig. 7A**). LCI assays further

confirmed that BU1 interacted with ILI1 or IBH1 (**Fig. 7B**, **7C**). ILI1 and IBH1 are both (b)HLH proteins, and reportedly antagonistically regulate BR signaling and leaf inclination in rice (Zhang et al., 2009a). To investigate how BU1 regulates BR signaling via ILI1 and IBH1, *ILI1* and *IBH1* knockout Kitaake lines were generated. Consistent with previous reports (Zhang et al., 2009a), the leaf inclination of *ILI1* knockout plants (*ili1*) is smaller than that of the wild type, while the leaf inclination of *IBH1* knockout plants (*ibh1*) is larger (**Fig. 7D-7G, Supplementary Figure S21**). To further investigate genetic relationships between *BU1* and *IBH1*, or *BU1* and *ILI1*, *bu1/ibh1* and *bu1/ili1* double mutants were generated. Compared to WT, the flag leaf inclination of both *bu1/ibh1* and *bu1/ili1* double mutants was close to that of *ibh1* and *ili1* single mutants (**Fig. 7D-7G**). These results indicate that *BU1* likely functions genetically upstream of *ILI1* and *IBH1* in the same genetic pathway in the regulation of BR signaling in rice.

BU1 and ILI1 synergistically relieve IBH1-repressed expression of *OsARF11*

To further investigate how BU1, ILI1, and IBH1 jointly regulate BR signaling, we aimed to identify a common target gene regulated by these factors. DAP-seq analysis was performed using IBH1-His proteins. Two replicates were conducted, and coenrichment of the *OsARF11* promoter region was observed in both samples (**Supplementary Figure S22A**). And IBH1 mainly bound to a motif containing GA-repeats in the *OsARF11* promoter region (**Supplementary Figure S22B**). ChIP-qPCR and EMSAs further confirmed direct binding of IBH1 to the promoter of *OsARF11* (**Fig. 8A**, **8B**). *OsARF11* is the rice homolog of Arabidopsis *ARF5*/*MONOPTEROS*, and loss of its function results in reductions in the root system, panicle branches, and grains, and an erect leaf phenotype. Besides its role in auxin signaling, OsARF11 also positively regulates the BR signaling pathway by directly activating *BRI1* expression (Sakamoto et al., 2013; Dastidar et al., 2019; Sims et al., 2021). To confirm this, two *OsARF11* mutants (*osarf11-1,2*) of Kitaake were generated (**Supplemental Fig. S23F**), and compared to WT plants both mutants exhibited significantly reduced flag leaf inclination (**Supplementary Figure S23A**, **23B**), and reduced sensitivity to BL

treatment (**Supplementary Figure S23C**, **23D**). *OsARF11* expression was rhythmically induced by BL, exhibiting two peaks of high expression at 0.5 hours and 9 hours during BL treatment (**Supplementary Figure S23E**). These findings suggest that *OsARF11* might be the downstream gene co-regulated by IBH1, BU1, and ILI1.

Additional analyses were conducted to investigate the regulatory roles of BU1, ILI1, and IBH1 in the modulation of *OsARF11* transcription. In quantitative transactivation assays, IBH1-GFP significantly repressed the luciferase activity driven by *ProOsARF11-min35S:LUC*. This repressive effect was counteracted by BU1-FLAG or ILI1-FLAG, and was more effectively counteracted by the combination of BU1-FLAG and ILI1-FLAG (**Fig. 8C** and **8D**). EMSAs indicated that IBH1—but not ILI1 or BU1—could bind to the promoter of *OsARF11*, and BU1 or ILI1 alone slightly, and BU1 and ILI1 together further inhibited IBH1 binding to the *OsARF11* promoter (**Fig. 8E**). *OsARF11* expression levels were upregulated in *ibh1-1* and *ibh1-2* mutants, but downregulated in *bu1* and *ili1* single mutants, and greater downregulation was evident in *bu1/ili1* double mutants (**Fig. 8F and 8G**). These results indicate a synergistic effect of BU1 and ILI1 in antagonizing the IBH1-repressed transcription of *OsARF11*.

To test whether ILI1, IBH1, and BU1 could form a heterotrimer to enhance their interaction, an *in vitro* pull-down assay was performed. The addition of increasing amounts of ILI1-GST did not enhance interaction between IBH1 and BU1 (**Supplementary Figure S24**). In a previous report fluorescence of eGFP-BU1 was mainly distributed in the cytoplasm of rice coleoptile cells (Tanaka et al., 2009), thus we repeated the experiment in Kitaake protoplasts. Consistent with that previous report BU1-GFP fluorescence was mainly distributed in the cytoplasm with a relatively weak nuclear localization signal, whereas IBH1-GFP was localized in the nucleus, and ILI1-GFP was localized in both the nucleus and the cytoplasm (**Supplementary Figure S25A**). Similar subcellular localization patterns of ILI1-GFP, IBH1-GFP, and BU1-GFP were also observed in leaf epidermal cells of *N. benthamiana* (**Supplementary Figure S25A**). Interestingly, when BU1-GFP and ILI1-FLAG proteins were co-expressed in the epidermal cells of *N. benthamiana* leaves, there

was an increased nuclear BU1-GFP fluorescence signal (**Fig. 8H**). Consistent with this, in western blotting analysis the BU1-GFP band was faint without ILI1, but became distinct in the presence of ILI1 in the cell nucleus of *N. benthamiana* leaves (**Fig. 8I**). Similarly, the subcellular localization signal of BU1-GFP alone was mainly distributed in the cytoplasm of Kitaake or *ili1* protoplasts (**Fig. 8J, Supplementary Figure S25B**), and co-expression of BU1-GFP and ILI1-FLAG in Kitaake protoplasts also increased nuclear BU1-GFP fluorescence signals (**Fig. 8K–8L**). These findings indicate that the presence of ILI1 facilitates the translocation of BU1 from the cytoplasm to the nucleus.

Discussion

In animals and plants, heterotrimeric G-proteins transmit extracellular signals into intracellular signaling components (Gilman, 1987; Urano et al., 2013). However, the precise interplay between G protein components and BR signaling in rice remains largely unexplored. Herein we report that the DEP1-GNA-OsMYB86-BU1/ILI1/IBH1-*OsARF11* pathway links the Gγ subunit DEP1 to the BR signaling pathway. First, we found that *DEP1* transgenic plants exhibited BR-related phenotypes, while *dep1* mutants showed reduced BR sensitivity, and *DEP1-OE* plants exhibited increased BR sensitivity (**Fig. 1**). Second, BRs facilitated the nuclear import of DEP1 via the BR signaling protein GNA (**Fig. 2, Supplementary Figure S6**). Third, we showed that DEP1 interacts with OsMYB86, a MYB transcription factor that positively regulates BR signaling, and that both are in the same genetic pathway that regulates leaf inclination in rice (**Fig. 3-6**). Fourth, we revealed that DEP1 boosts the OsMYB86-promoted transcription of *BU1* with the help of GNA (**Fig. 6**). Fifth, we found that by interacting with BU1, ILI1 promotes the importation of BU1 into the nucleus, where they synergistically and efficiently relieve the IBH1-repressed transcription of OsARF11 (**Fig. 7 and Fig. 8**), a gene involved in both auxin and BR signaling. Lastly, we found that the function of the DEP1-OsMYB86-BU1 pathway in BR signaling is likely dependent on RGA1 (**Supplementary Figure S20**) (Wang et al., 2006; Tanaka et al., 2009; Sun et al., 2018).

However, the precise mechanism underlying RGA1's regulation in the DEP1-OsMYB86-BU1 pathway remains unclear and requires further research.

Recently, we found that GNA interacts with DEP1 and facilitates its entry into the cell nucleus (Zhang et al., 2024). Here, we further confirmed that in the presence of GNA and BR, the nuclear entry of DEP1 proteins was more effectively promoted (**Fig. 2, Supplementary Figure S6**). Notably, GNA is a GRAS family protein that has been shown to possess an innate capability to activate RNA polymerase (Hirsch et al., 2009). Therefore, upon entering the cell nucleus, DEP1 interacts with BR signaling-related transcription factors such as OsMYB86 (**Fig. 3**) and GNA (Zhang et al., 2024), potentially forming a transcriptional regulatory complex to efficiently promote the transcription of a key downstream gene *BU1* (**Fig. 6F**). Because we were unable to detect DEP1 through Western blot analysis in *35S:DEP1-GFP* transgenic plants, as observed in both our study and previous reports (Taguchi-Shiobara et al., 2011; Sun et al., 2018), our conclusions that BRs promote DEP1's nuclear localization are primarily based on transient expression systems. This limits further investigation into the roles of the rice G-protein complex in *planta*. Therefore, identifying the underlying reasons for the undetectable DEP1 in transgenic plants is valuable for a comprehensive understanding of the detailed roles of DEP1 in rice plants.

The bHLH superfamily is a transcription factor family containing many members, and it is widely found in both plants and animals (Hao et al., 2021). Many members of the bHLH family have been implicated in BR signaling in rice, including BU1 (Tanaka et al., 2009), ILI1, IBH1 (Zhang et al., 2009a), OsBUL1 (Jang et al., 2017), OsbHLH98 (Guo et al., 2021), and OsbHLH92 (Teng et al., 2023). Based on the phylogenetic relationship and DNA motif binding capacities of bHLH family members, six major groups have been identified within the bHLH family. IBH1 is not included in any of the six major groups however, and its DNA-binding capacity and preferred binding motif are unknown (Hao et al., 2021). In addition, although we discover a mechanism by which DEP1, GNA and OsMYB86 activate the expression of *BU1*, how BU1 together with ILI1 and IBH1 transmits BR signal remains unclear. By further investigations, we found that IBH1

directly repressed the expression of *OsARF11*, a gene involved in BR and auxin crosstalk (Sakamoto et al., 2013), by binding to the GA-repeat sequences in the *OsARF11* promoter. With respect to the specific mechanism by which they regulate BR signaling, ILI1 likely facilitates the importation of BU1 into the nucleus where together they synergistically and efficiently inhibit binding of IBH1 to the promoter of *OsARF11*, thus attenuating the IBH1-repressed transcription of *OsARF11*, finally promoting BR signaling (**Fig. 8**, **Supplementary Figure S22, S24, S25**). These results enhance our understanding of the regulatory mechanism of BR signaling by HLH/bHLH proteins.

As well as BR, auxin is an important hormone that regulates rice leaf inclination, and the genes involved in the auxin synthesis and signaling pathway affect rice leaf inclination (Zhang et al., 2009b; Bian et al., 2012; Huang et al., 2021). Among the auxin-related genes affecting rice leaf inclination, auxin-responsive factors (ARFs) have been extensively reported to regulate rice leaf inclination by mediating crosstalk between auxin and BR. For example, some ARFs such as OsARF1 and OsARF4 act as negative regulators of BR signaling, inhibiting rice leaf inclination by mediating crosstalk between auxin and BR (Song et al., 2009; Qiao et al., 2022). In contrast, other ARFs such as OsARF11 and OsARF19 positively regulate rice leaf inclination by promoting the transmission of BR signaling (Sakamoto et al., 2013; Zhang et al., 2015b). In the present study BU1, ILI1, and IBH1 converged and directly controlled *OsARF11* expression (**Fig. 8**), which provides insights into the key role of auxin in regulating leaf inclination and crosstalk between auxin and BR.

Based on the above findings, we propose the following working model (**Fig. 9**). RGA1, acting as a key signaling switch, triggers BR signaling by activating the DEP1-mediated pathway in rice. As BR levels increase in the plant, BRs promote the accumulation of GNA proteins, which in turn facilitate the nuclear entry of DEP1. In the nucleus, DEP1 interacts with OsMYB86 and GNA, likely forming a transcriptional regulatory complex to effectively activate OsMYB86-mediated transcription of *BU1*. Additionally, BRs promote the expression of the BR positive response gene

ILI1, while repressing the BR negative response gene *IBH1*. The ILI1 protein then interacts with BU1, facilitating the transfer of BU1 from the cytoplasm to the nucleus, where together they inhibit IBH1's binding to the promoter of *OsARF11*. This relieves IBH1-mediated repression of *OsARF11* transcription, thereby activating BR responses and increasing leaf inclination in rice. These findings suggest that the BR signaling pathway mediated by DEP1 effectively activates BR responses in rice. This offers insights into the mechanisms of BR signaling and provides a theoretical basis for breeding rice cultivars with optimal leaf inclination for dense planting.

Materials and Methods

Plants and growth conditions

To generate *dep1*, *osmyb86*, *d1*, *bu1*, *ili1*, *ibh1*, and *osarf11* knockout plants, 20-bp gene-specific spacer sequences of *DEP1*, *OsMYB86*, *RGA1*, *BU1*, *ILI1*, *IBH1*, and *OsARF11* were inserted into the sgRNA/Cas9 construct, respectively (Miao et al., 2013). To generate a *DEP1* overexpression construct, the full-length coding sequence of *DEP1* was cloned into the binary vector pCAMBIA1305GFP to produce *Pro35S:DEP1-GFP*. The full-length coding sequence of *OsMYB86* was amplified and cloned into the binary vectors pCUbi1390, pCAMBIA2300, and pCAMBIA1305 to produce *OsMYB86* overexpression constructs *ProUbi:OsMYB86*, *ProActin:OsMYB86*, and *Pro35S:OsMYB86-GFP*. The above constructs were introduced into *Agrobacterium tumefaciens* strain EHA105, then transformed into the callus of the *japonica* cultivar variety, Kitaake. To obtain *OsMYB86-OE/bu1* plants the callus of Kitaake was transformed with a mix of *A. tumefaciens* containing *ProActin:OsMYB86* and *bu1-sgRNA/Cas9* constructs. *ProUbi:OsMYB86* and *bu1* plants were crossed to obtain *OsMYB86-OE/bu1* plants. *ProActin:BU1* and *osmyb86-3* plants were crossed to obtain *BU1-OE/osmyb86-3* plants. *Pro35S:DEP1-GFP* and *osmyb86-3* plants were crossed to obtain *DEP1-OE/osmyb86-3* plants. *ProUbi:OsMYB86* and *dep1-1* plants were crossed to obtain *OsMYB86-OE/dep1-1* plants. *ProUbi:OsMYB86* and *d1* plants were crossed to obtain *OsMYB86-OE/d1* plants. *bu1* and *ibh1* plants were crossed to obtain

bu1/ibh1 plants. *bu1* and *ili1* plants were crossed to obtain *bu1/ili1* plants. All plants were grown in the experimental field of the Chinese Academy of Agricultural Sciences under natural conditions with conventional management. The detailed primer information is provided in the **Supplementary Table S1.**

Subcellular localization

For subcellular localization of DEP1, OsMYB86, BU1, ILI1, and IBH1 protein, the full-length coding sequences of *DEP1*, *OsMYB86*, *BU1*, *ILI1*, and *IBH1* were amplified and cloned into the transient expression vector pAN580 to generate *Pro35S:DEP1/OsMYB86/BU1/ILI1/IBH1-GFP* fusion plasmids. The *Pro35S:DEP1/OsMYB86/BU1/ILI1/IBH1-GFP* fusion plasmids were transformed into rice protoplasts as previously described (Zhang et al., 2011). After incubation at 25°C for 6–16 hours, fluorescence detection was performed. Full-length coding sequences of *DEP1*, *OsMYB86*, *BU1*, *IBH1*, and *ILI1* were cloned into pCAMBIA1305 to generate *Pro35S:DEP1/OsMYB86/BU1/ILI1/IBH1-GFP* fusion plasmids. The vectors were introduced into *A. tumefaciens* strain EHA105, then *N. benthamiana* leaves were exposed to specific combinations. Fluorescent signals were monitored 48–72 h after exposure. *p35S:D53-mCherry* was used as a nucleus marker (Zhou et al., 2013), *Pro35S:SLG-mCherry* was used as a nucleus and cytoplasm marker (Feng et al., 2016). Fluorescence signals were observed via a Zeiss LSM980 confocal microscope.

Subcellular localization analysis of DEP1

To investigate the effects of BL on DEP1-GFP localization in *N. benthamiana* leaf epidermal cells, a final concentration of 2 μM of 2,4-epiBL mixed with Agrobacterium-containing mediator solution was used for infiltration into *N. benthamiana* leaves. The same volume of ethanol mixed with Agrobacterium-containing mediator solution was used as a control. Fluorescent signals were monitored 60-72 h after infiltration.

Subcellular localization analysis of BU1

To investigate the effects of ILI1 on BU1 localization Kitaake protoplasts were transformed with *Pro35S:BU1-GFP* with free FLAG and *Pro35S:ILI1-FLAG*, respectively, or *ili1* protoplasts were transformed with free FLAG. Fluorescent signals were monitored 48–72 h after infiltration. The signal intensity of BU1-GFP in the nucleus and the signal intensity of the entire cell were quantified via ZEN 3.1 (blue edition) to calculate the percentage of BU1 signal in the nucleus.

Yeast two-hybrid assay

The coding region of *DEP1* was fused to the GAL4 binding domain of the pGBKT7 vector as a bait. A cDNA library from young rice inflorescences was used to perform Y2H screening, and positive clones were identified via sequencing. Full-length coding sequences of *RGB1*, *RGA1*, *GGC2*, *GS3*, and *BU1* and various truncated versions of *DEP1* were cloned into pGBKT7. Full-length coding sequences of *OsMYB86*, *ILI1*, and *IBH1* were cloned into pGADT7. pGADT7-DLT, pGBKT7-DLT, and pGBKT7-RGA1 were used as negative controls. Various combinations of plasmids were cotransformed into the yeast strain AH109 (Clontech). After growing on SD-Trp/-Leu plates for 3 d at 30°C, interactions were observed on the selective medium SD-Leu/-Trp/-His/-Ade.

BiFC assay

Full-length coding sequences of *OsMYB86* and *DEP1* were fused to p2YC and p2YN vectors, respectively. The plasmids were transformed into *A. tumefaciens* (strain EHA105) and infiltrated into *N. benthamiana* leaves as previously described (Waadt and Kudla, 2008). P2YN-RGA1 and P2YC-DLT were used as negative controls. Fluorescent signals were monitored 48–72 h after infiltration via a Zeiss LSM980 confocal microscope.

LCI assay

Full-length coding sequences of *OsMYB86*, *IBH1*, and *ILI1* were fused to the pCAMBIA1300-Cluc vector. Full-length coding sequences of *DEP1* and *BU1* were fused to the pCAMBIA1300-nLUC vector. The vectors were introduced into *A. tumefaciens* strain EHA105, then infiltrated into *N. benthamiana* leaves. RGA1-nLUC, DLT-nLUC, and DLT-cLUC were used as negative controls. ILI1-nLUC and IBH1-cLUC were used as positive controls. After 36–48 h, *Nicotiana benthamiana* leaves were treated with 1 mm luciferin (E1601, Promega) for 3 mins, then the luciferase activities were measured using an imaging apparatus (LB 985, Berthold).

ChIP-seq and ChIP-qPCR

ChIP-seq assays were conducted by SeqHealth (Wuhan, China) using the leaves, stems, and lamina joints of *Pro35S:OsMYB86-GFP* transgenic plants, with two biological replicates. Anti-GFP antibodies (598-7, Medical Biological Laboratories) were used, and the sequencing depth was set at 20 million reads per sample. Raw sequencing data were filtered using Trimmomatic (version 0.36) to remove low-quality reads and trim adapter sequences. Read distribution analysis was performed with RSeQC (version 2.6), and peak calling was conducted using MACS2 (version 2.1.1). Peak annotation and distribution analysis were performed using bedtools (version 2.25.0). Differential binding peaks were identified via a Fisher's test using a custom Python script. Motif analysis was conducted using Homer (version 4.10). Gene Ontology (GO) and Kyoto Encyclopedia of Genes and Genomes (KEGG) enrichment analyses for annotated genes were performed using KOBAS (version 2.1.1), with a corrected p value threshold of 0.05 to determine statistically significant enrichment. ChIP-qPCR assays were performed as previously described (Wang et al., 2018). Leaves, stems, and lamina joints of *Pro35S:OsMYB86-GFP* transgenic plants or young *Nicotiana benthamiana* leaves cotransformed with the *Pro35S:OsMYB86-GFP* and *ProBU1:LUC* vectors were used to test the enrichment of OsMYB86 at the promoter regions of *BU1*. Young *N. benthamiana* leaves cotransfected with *Pro35S:IBH1-GFP* and

ProOsARF11:LUC vectors were used to test the enrichment of *IBH1* in the promoter regions of *OsARF11*. GFP antibodies (Medical Biological Laboratories, 598) were used for detection.

LUC activity assay

An approximately 2.5-kb promoter region of *BU1* and *OsARF11* was cloned to fuse into the pGreenII0800-LUC vector to generate *ProBU1:LUC* and *ProOsARF11:LUC* reporters. Full-length coding sequences of *OsMYB86* and *IBH1* were cloned to fuse into the pCAMBIA1305GFP vector to generate Pro35S:OsMYB86-GFP and Pro35S:IBH1-GFP effectors. Full-length coding sequences of *DEP1*, *GNA*, *ILI1*, and *BU1* were cloned to fuse into the pCAMBIA1300-FLAG vector to generate *Pro35S:DEP1-FLAG*, *Pro35S:GNA-FLAG*, *Pro35S:ILI1-FLAG*, and *Pro35S:BU1-FLAG* effectors. Empty vectors were used as negative controls. The combined reporter and effector plasmids were cotransformed into rice protoplasts. Various combinations of plasmids were also cotransformed into *A. tumefaciens* (strain EHA105) then infiltrated into *N. benthamiana* leaves. LUC activity was quantified with a Dual-Luciferase Assay Kit (Promega) in accordance with the manufacturer's instructions, and relative LUC activity was calculated as the ratio of LUC/REN.

EMSA

To perform EMSAs, full-length coding sequences of *OsMYB86* and *DEP1* were cloned into the pMAL-c2x vector. Full-length coding sequences of *ILI1*, *IBH1*, and *BU1* were cloned into pGEX4T-1. The correct constructs of *MBP-OsMYB86*, *MBP-DEP1*, *ILI1-GST*, *BU1-GST*, *IBH1-GST*, and empty *MBP* and *GST* vectors were introduced into the *Escherichia coli* strain DE3 to induce protein expression. MBP and MBP-labeled protein were eluted with 10 mM maltose. GST and GST-labeled protein were eluted with 20 mM glutathione. Oligonucleotide probes were synthesized and labeled with biotin by Thermo Fisher Scientific. EMSA was then performed using the lightshift Chemiluminescent EMSA Kit (Thermo, 20148).

RNA extraction and RT-qPCR analysis

Total RNA was extracted from lamina joints of 70-day-old plants and 2-week-old BL treatment seedlings using the ZR Plant RNA MiniPrep Kit (Zymo Research) in accordance with the manufacturer's instructions. Total RNAs were reverse transcribed using a Reverse Transcription Kit (Qiagen). RT-qPCR analyses were performed using an ABI 7500 realtime PCR system with a SYBR Premix Ex Taq II Kit (Takara). The rice *Ubiquitin* (*UBQ*) gene was used as an internal control.

Co-IP assay

To detect OsMYB86-DEP1 interaction *in vivo*, full-length coding sequences of *DEP1* and *OsMYB86* were cloned into pCAMBIA1305.1-GFP and pCAMBIA1300-FLAG vectors, respectively. The plasmids were cotransformed into *A. tumefaciens* (strain EHA105) then infiltrated into *N. benthamiana* leaves. After 48 h treatment, total protein was extracted from infiltrated *N. benthamiana* leaves. Anti-GFP (598-7, Medical Biological Laboratories, 1:5000) and anti-FLAG antibodies (M185-7, Medical Biological Laboratories, 1:5000) were used in immunoblotting analysis.

BL treatment

BL was dissolved in ethanol. For the lamina inclination test, approximately 14-day-old rice seedlings with expanded third leaves were soaked in rice nutrient solution supplemented with different concentrations of 2,4-epiBL. Ethanol was used as a mock treatment. Images of plants were then taken for lamina inclination measurement at 24-48 h after treatment, and lamina inclination was measured using ImageJ software. The coleoptile length test was performed as previously described (Tong and Chu, 2017). Seeds were sterilized and germinated on 1% agar medium containing different concentrations of BL. After 7 days of growth at 30°C the length of

coleoptiles was measured.

Flag leaf inclination observation and measurement

After the rice's main panicle had fully emerged, uniform samples were collected by cutting segments that included the panicle, leaf lamina joint, and leaf blade. Photographs were then taken, and blade inclinations were measured using ImageJ software.

Phylogenetic analysis

Gene sequences used in phylogenetic analysis were downloaded from https://phytozome-next.jgi.doe.gov/, and a phylogenetic tree was constructed using MEGA5 software and the neighbor-joining method with 1,000 bootstrap replicates. The sequences used to construct the phylogenetic tree are provided in **Supplementary Data Set S2.**

***In vitro* pull-down assay**

Full-length coding sequences of *IBH1*, *ILI1*, and *BU1* were cloned into the expression vectors pET-28a, pGEX4T-1, and pMAL-c2x, respectively, to generate His, GST, and MBP tag fusion proteins. IBH1-His, ILI1-GST, GST, BU1-MBP, and MBP proteins were then expressed in the *E. coli* strain BL21 (DE3) (TransGen) under induction with 0.5 mM isopropyl-b-D-thiogalactoside, and shaking at 16°C for 16 h. Fusion proteins were purified using GST magnetic beads (BEAVER), His magnetic beads (BEAVER), or amylose magnetic beads (Biolabs) in accordance with the manufacturer's instructions. To detect BU1-ILI1-IBH1 interaction using the *in vitro* pull-down assay, approximately equal amounts of GST and GST-ILI1 or MBP and MBP-BU1 were mixed with His-IBH1, then the mixed supernatants were incubated with 30 μL of His magnetic beads in 1.5 mL phosphate-buffered saline. After incubation for 60 min the beads were washed six times with phosphate-buffered saline, then boiled with 100 μL protein loading buffer at 100°C for 10 min. The proteins were separated in 10% SDS-PAGE gels and detected via western blotting using

anti-GST antibody (PM013-7, Medical Biological Laboratories, 1:5000), anti-His antibody (D291-7, Medical Biological Laboratories, 1:5000), and anti-MBP antibody (E8032S, BioLabs, 1:5000).

Fractionation of proteins and immunoblotting

Protein fractionation and immunoblotting assays for *N. benthamiana* were performed using a commercial nucleus/cytoplasm separation kit (Beyotime P0028) according to the manufacturer's instructions. For rice protoplast protein fractionation and immunoblotting assays, prepare a sufficient amount of rice protoplasts. Centrifuge 250 × g of the sample for 5 minutes to collect the protoplasts, discard the supernatant, and retain the pellet. Resuspend the pellet in cytoplasmic protein extraction reagent (Beyotime P0028), vortex for 5 s, incubate on ice for 10 min, and centrifuge at 12,000 × g for 10 min at 4°C. Carefully collect the supernatant to obtain cytoplasmic proteins. Prepare 60% and 30% sucrose solutions using the cytoplasmic protein extraction reagent and slowly layer them sequentially into a centrifuge tube. Resuspend the crude nuclear pellet in the cytoplasmic protein extraction reagent and gently load it onto the top of the sucrose gradient. Centrifuge at 20,000 × g for 2 h at 4°C. Carefully collect the white interface between the 30% and 60% sucrose layers and resuspend it in nuclear protein extraction reagent (Beyotime P0028) to obtain nuclear proteins. Full-length coding sequences of *DEP1* and *BU1* were cloned into pCAMBIA1305.1-GFP vector. Full-length coding sequences of *GNA* and *ILI1* were cloned into pCAMBIA1300-FLAG vector. The plasmids were cotransformed into *A. tumefaciens* (strain EHA105), then infiltrated into *N. benthamiana* leaves. 60-72 hours after infiltration, 0.5 g *N. benthamiana* leaves were harvested for subsequent experiments. Full-length coding sequences of *DEP1*was amplified and cloned into the transient expression vector pAN580 to generate *Pro35S:DEP1-GFP* fusion plasmids. The *Pro35S:DEP1-GFP* fusion plasmids were transformed into rice protoplasts as previously described (Zhang et al., 2011). After incubation at 25°C for 12 hours, protoplasts were harvested for subsequent experiments. Twenty microliters of cytoplasmic or nuclear fractions were used in immunoblot analysis performed with anti-GFP (598-7, Medical

Biological Laboratories, 1:5000), anti-H3 (ab1791, abcam, 1:1000), anti-β-actin (BE0033, Easybio, 1:1000), and anti-actin (AC009, ABclonal, 1:1000).

Statistical analysis

The statistical results are indicated as means±SD, where n represents the number of biological replicates. GraphPad Prism 5.0 was used for statistical analysis. Detailed statistical analysis data are provided as Supplementary Data Set 1.

Accession numbers

Sequences of genes involved in this study can be found in Rice Genome Annotation Project https://rice.uga.edu/, and Phytozome https://phytozome-next.jgi.doe.gov/ under the accession numbers LOC_Os09g26999(DEP1), LOC_Os03g51330(GNA), LOC_Os01g50720(OsMYB86), LOC_Os06g12210(BU1), LOC_Os04g54900(ILI1), LOC_Os04g56500(IBH1), LOC_Os05g26890(RGA1), LOC_Os04g56850(OsARF11), LOC_Os06g03710(DLT), LOC_Os03g46650(RGB1), LOC_Os09g32510(OsbHLH92), LOC_Os01g10040(D2), LOC_Os04g39430(D11), LOC_Os03g40540(BRD1), LOC_Os10g25780(BRD2), LOC_Os02g47280(OsGRF4), LOC_Os05g39950(OsOFP22). Sequencing data of ChIP-seq and RNA-seq can be found in NCBI https://www.ncbi.nlm.nih.gov/ (Bioproject, PRJNA1159116, ChIP-seq) (Bioproject, PRJNA1159124, PRJNA1211729, RNA-seq).

Author contributions

Jianmin Wan and Zhijun Cheng supervised the project; Shuai Li and Qibing Lin designed the research and wrote the paper; Zhijun Cheng and Zhichao Zhao performed most of the plant hybridization experiments; Tianzhen Liu provided the plant material of OsMYB86; Jinhui Zhang provided the plant material of GNA. Shuai Li performed most of the experiments; Xinxin Xing

prepared the rice protoplasts; Xin Liu provided technical assistance of the ChIP assay and bioinformatics analysis; Miao Feng, Sheng Luo, Kun Dong, Yupeng Wang, Feng Zhang, Jian Wang, Rong Miao, Wenfan Luo, Cailin Lei, Yulong Ren, Shanshan Zhu, Xin Wang provided technical assistance; Xiuping Guo generated the transgenic plants.

Funding

This research was supported by Biological Breeding-National Science and Technology Major Project (2024ZD04080), the Agricultural Science and Technology Innovation Program (CAAS-ZDRW202401), and the National Key Research and Development Program of China (2022YFF1002900, 2022YFD1200104).

Competing interests

The authors declare no competing interests.

Figure Legends

Figure 1. DEP1 is a positive regulator of BR signaling.

(**A**) Plant phenotypes of Kitaake, *dep1-1, dep1-2* and *DEP1-OE* at mature stage. Bar = 15 cm.

(**B**) Phenotypes and measurements of the flag leaf inclination of Kitaake, *dep1-1, dep1-2* and *DEP1-OE* at mature stage. Asterisks indicate significant difference compared with Kitaake. Data = means ± SD (n = 12, **P < 0.01, Student's *t*-test). Bar = 4 cm (applies to all images in Panel B).

(**C**) and (**D**) Phenotypes and measurements of the grain length of Kitaake, *dep1-1, dep1-2* and *DEP1-OE*. Asterisks indicate significant difference compared with Kitaake. Data = means ± SD (n = 20, **P < 0.01, Student's *t*-test). Bar = 10 mm.

(**E**) Lamina bending analysis of Kitaake, *dep1-1*, *dep1-2* and *DEP1-OE* at the seedling stage in response to BL (brassinolide). Bar=4 cm (applies to all images in Panel E)

(**F**) Quantification of the lamina inclination bending assay in (**E**) in response to different concentrations of BL. Data = means ± SD. The percentages indicate the promoting effect of BL on lamina inclination. Different letters indicate significant differences as determined by Tukey's multiple comparisons test (P < 0.05, n = 14).

(**G**) The expression change pattern of *DEP1* in response to 1 μM BL. Data = means ± SD. Ethanol was used as a mock treatment. The different letters above the histogram indicate significant differences (p < 0.05) by Tukey's multiple comparison test. (n = 3).

Figure 2. BRs promote DEP1 nuclear entry through GNA.

(**A**) Three localization patterns of DEP1-GFP in Nipponbare protoplasts. Type I, cytoplasmic and membrane localization without nuclear localization signals of DEP1-GFP. Type II, cytoplasmic and membrane localization with nuclear membrane outline. Type III, cells with evident nuclear localization.

(**B**) Two localization patterns of DEP1-GFP in *brd1* mutant protoplasts.

(**C**) Two localization patterns of DEP1-GFP co-expressed with GNA in *brd1* mutant protoplasts.

(**D**) The proportion of DEP1-GFP localization in different expression combinations. 100 cells were counted for each expression combination.

(**E**) The nuclear and cytoplasmic distribution of DEP1-GFP in different expression combinations. Histone 3 and Actin were used as markers for the nucleus and cytoplasm, respectively. C, cytoplasmic fraction; N, nuclear fraction.

D53-mCherry, a nuclear marker. Bar = 10 μm.

Figure 3. DEP1 interacts with OsMYB86

(**A**) OsMYB86 interacts with DEP1, GS3, and GGC2, but not with RGA1 or RGB1 in yeast cells. SD-Leu-Trp, selective medium lacking Leu and Trp. SD-Leu-Trp-Ade-His, lacking Trp, Leu, His, and Ade. pGADT7-DLT and pGBKT7-RGA1 were used as the negative controls.

(**B**) BiFC assay verifies the interaction between DEP1 and OsMYB86 in the leaf epidermal cells of *N. benthamiana*. P2YN-RGA1 and P2YC-DLT were used as the negative controls. Arrowheads represent nuclear localization. Bar = 50 μm.

(**C**) LCI assay verifies that DEP1 interacts with OsMYB86 in the leaf epidermal cells of *N. benthamiana.* RGA1-nLUC and DLT-cLUC were used as the negative controls. ILI1-nLUC and IBH1-cLUC were used as the positive controls. Colored scale bar indicates the luminescence intensity in CPS.

(**D**) Co-IP analysis of the interaction between DEP1-GFP and OsMYB86-FLAG in the leaf epidermal cells of *N. benthamiana*. IB, immunoblotting analysis. kDa, kilodaltons.

Figure 4. OsMYB86 positively regulates BR signaling as a BR-responsive factor.

(**A**) Plant phenotypes of Kitaake, *osmyb86-1, osmyb86-2* and *osmyb86-3* at mature stage. Bar = 15 cm.

(**B**) Plant phenotypes of Kitaake, *OsMYB86-OE-1, OsMYB86-OE-2* and *OsMYB86- OE-3* at mature stage. Bar = 15 cm.

(**C**) Phenotypes and measurements of the flag leaf inclination of Kitaake, *osmyb86-1, osmyb86-2, osmyb86-3*, *OsMYB86-OE-1, OsMYB86-OE-2* and *OsMYB86-OE-3* at mature stage. Asterisks indicate significant difference compared with Kitaake. Data = means ± SD (n = 15, **P < 0.01, *P < 0.05, Student's *t*-test). Bar = 4 cm (applies to all images in Panel C)

(**D**) Phenotypes and measurements of the grain length of Kitaake, *osmyb86-1, osmyb86-2, osmyb86-3*, *OsMYB86-OE-1, OsMYB86-OE-2* and *OsMYB86-OE-3*. Asterisks indicate significant difference compared with Kitaake. ns indicates no significance compared with Kitaake. Data = means ± SD (n = 10, **P < 0.01, *P < 0.05, Student's *t*-test). Bar = 10 mm.

(**E**) Lamina bending analysis of Kitaake, *osmyb86-1, osmyb86-3*, *OsMYB86-OE-1* and *OsMYB86-OE-2* at the seedling stage in response to BL. Bar = 4 cm (applies to all images in Panel E)

(**F**) Quantification of the lamina inclination bending assay in (**E**) in response to different concentrations of BL. Data = means ± SD. The percentages indicate the promoting effect of BL on lamina inclination. Different letters indicate significant differences as determined by Tukey's multiple comparisons test (P < 0.05, n = 15).

(**G**) The expression change pattern of *OsMYB86* in response to 1 μM BL. Ethanol was used as a mock treatment. Data = means ± SD. The different letters above the histogram indicate significant differences (p < 0.05) by Tukey's multiple comparison test. (n = 3).

Figure 5. OsMYB86 directly promotes *BU1* expression in rice.

(**A**) Overview of the number of genes associated with OsMYB86 binding sites in 2 ChIP-sequencing replicates. rep, replicate.

(**B**) Relative expression level of *BU1* in the lamina joint from 60-day-old Kitaake, *OsMYB86-OE-1* and *osmyb86-3*. Asterisks indicate significant difference compared with Kitaake. Data = means ± SD (n = 3, **P < 0.01, Student's *t*-test).

(**C**) Relative expression changes folds of *BU1* in the lamina joint from 14-day-old Kitaake, *OsMYB86-OE-1* and *osmyb86*-3 under 1 μM BL treatment. 0 h, 3 h, 6 h, 18 h and 24 h represent the treated time by BL. Data = means ± SD (n = 3).

(**D**) Diagram of the *BU1* promoter region. Asterisks: R2R3-MYB family transcription factors recognize elements ([C/T]NGTT[G/T]).

(**E**) ChIP-qPCR assays showing *in vivo* binding of OsMYB86 to the *BU1* promoter. Cross-linked chromatin samples were extracted from *Pro35S:OsMYB86-GFP* transgenic plants and then precipitated with anti-GFP antibody. Nb (No antibody) served as a negative control. Asterisks indicate significant differences as determined by Tukey's multiple comparisons test Data = means ± SD (n = 3, **P < 0.01, *P < 0.05).

(**F**) An EMSA shows that OsMYB86 binds directly to the [C/T]NGTT[G/T] motif in the *BU1* promoter. MBP protein, the negative control. The plus (+) and minus (-) signs denote the presence or absence of the protein and DNA probe in each sample.

(**G**) Plant phenotypes of Kitaake, *BU1-OE, osmyb86-3* and *osmyb86-3*/*BU1-OE* at mature stage. Bar = 15cm.

(**H**) Phenotypes and measurements of the flag leaf inclination of Kitaake, *BU1-OE, osmyb86-3* and *osmyb86-3*/*BU1-OE* at mature stage. Asterisks indicate significant difference compared with Kitaake. Data = means ± SD (n = 10, **P < 0.01, Student's *t*-test). Bar = 4 cm (applies to all images in Panel H)

(**I**) Plant phenotypes of Kitaake, *OsMYB86-OE, bu1* and *OsMYB86-OE/bu1* at mature stage. Bar = 15cm.

(**J**) Phenotypes and measurements of the flag leaf inclination of Kitaake, *OsMYB86-OE, bu1* and *OsMYB86-OE/bu1* at mature stage. Asterisks indicate significant difference compared with Kitaake. ns indicates no significance compared with Kitaake. Data = means ± SD (n = 10, **P < 0.01, Student's *t*-test). Bar = 4 cm (applies to all images in Panel J)

Figure 6. DEP1 acts upstream of OsMYB86 to boost OsMYB86 activated *BU1* transcription.

(**A**) Plant phenotypes of Kitaake, *DEP1-OE*, *osmyb86-3* and *DEP1-OE/osmyb86-3* at mature stage. Bar = 15cm.

(**B**) Phenotypes and measurements of the flag leaf inclination of Kitaake, *DEP1-OE*, *osmyb86-3* and *DEP1-OE/osmyb86-3* at mature stage. Asterisks indicate significant difference compared with Kitaake. ns indicates no significance compared with Kitaake. Data = means ± SD (n = 10, **P < 0.01, Student's *t*-test). Bar = 4 cm (applies to all images in Panel B)

(**C**) Plant phenotypes of Kitaake, *dep1-1, OsMYB86-OE* and *dep1-1/OsMYB86-OE* at mature stage. Bar = 15cm.

(**D**) Phenotypes and measurements of the flag leaf inclination of Kitaake, *dep1-1, OsMYB86-OE* and *dep1-1/OsMYB86-OE* at mature stage. Asterisks indicate significant difference compared with Kitaake. Data = means ± SD (n = 10, **P < 0.01, Student's *t*-test). Bar = 4 cm (applies to all images in Panel D)

(**E**) Effector and reporter constructs used in the dual luciferase assay.

(**F**) Representative of dual-luciferase reporter assay co-expressing in *Nicotiana benthamiana*. Co-expressing of *ProBU1:luc-Pro35S:Rluc* & *Pro35S:FLAG* & *Pro35S:GFP* are used as the control (Mock). Renilla luciferase (REN) is used as an internal control. The ratio of LUC/REN represents the relative activity of promoters. The different letters above the histogram indicate significant differences ($p < 0.05$) by one-way ANOVA followed by Tukey's multiple comparison test. Data = means ± SD (n = 4).

(**G**) Relative expression level of *BU1* in the lamina joint of Kitaake and *gna* transgenic lines. Asterisks indicate significant difference compared with Kitaake. Data = means ± SD (n = 3, **P < 0.01, Student's *t*-test).

(**H**) Relative expression level of *BU1* in the lamina joint from 60-day-old Kitaake and *dep1-1* transgenic lines. Asterisks indicate significant difference compared with Kitaake. Data = means ± SD (n = 3, **P < 0.01, Student's *t*-test).

(**I**) Relative expression changes folds of *BU1* in the lamina joint from 16-day-old Kitaake, and *dep1-1* under 1 μM BL treatment. 0 h, 3 h, 6 h, 9 h and 12 h represent the treated time by BL. Data = means ± SD (n = 3).

(**J**) An EMSA shows that DEP1 and GNA do not enhance the binding activity of OsMYB86 to the *BU1* promoter. GST and MBP proteins were used as negative controls. The plus (+) and minus (-) signs denote the presence or absence of the protein and DNA probe in each sample.

Figure 7. BU1 interacts with and functions upstream of IBH1 and ILI1.

(**A**) BU1 interacts with IBH1 and ILI1 in yeast cells. SD-Leu-Trp, selective medium lacking Leu and Trp. SD-Leu-Trp-Ade-His, lacking Trp, Leu, His, and Ade. pGADT7-DLT and pGBKT7-DLT were used as the negative control.

(**B**) and (**C**) LCI assays verify that BU1 interacts with IBH1 (**B**) or ILI1 (**C**) in the leaf epidermal cells of *N. benthamiana*. DLT-nLUC and DLT-cLUC were used as the negative control. ILI1-nLUC and IBH1- cLUC were used as the positive control. Colored scale bar indicates the luminescence intensity in CPS.

(**D**) Plant phenotypes of Kitaake, *bu1*, *ibh1* and *bu1*/*ibh1* at mature stage. Bar = 15 cm.

(**E**) Phenotypes and measurements of the flag leaf inclination of Kitaake, *bu1*, *ibh1* and *bu1*/*ibh1* at mature stage. Asterisks indicate significant difference compared with Kitaake. Data = means ± SD (n = 10, **P < 0.01, Student's *t*-test). Bar = 4 cm. (applies to all images in Panel E).

(**F**) Plant phenotypes of Kitaake, *bu1*, *ili1* and *bu1*/*ili1* at mature stage. Bar = 15cm.

(**G**) Phenotypes and measurements of the flag leaf inclination of Kitaake, *bu1*, *ili1* and *bu1*/*ili1* at mature stage. Asterisks indicate significant difference compared with Kitaake. Data = means ± SD (n = 10, **P < 0.01, Student's *t*-test). Bar = 4 cm. (applies to all images in Panel G). Figure 7E and 7G presents statistical data from the same year.

Figure 8. BU1 and ILI1 synergistically relieve the IBH1-repressed transcription of *OsARF11*.

(**A**) ChIP-qPCR assays showing *in vivo* binding of IBH1 to the *OsARF11* promoter. Nb (No antibody) served as a negative control. Data = means ± SD; asterisks indicate significant differences as determined by Tukey's multiple comparisons test (n = 3, **P < 0.01, *P < 0.05).

(**B**) An EMSA shows that IBH1 binds directly to the GA-repeats motif in the *OsARF11* promoter. GST protein, the negative control. The plus (+) and minus (-) signs denote the presence or absence of the protein and DNA probe in each sample.

(**C**) Effector and reporter constructs used in the dual luciferase assay. IBH1-GFP, BU1-FLAG and ILI1-FLAG were used as effectors, and GFP and 3 × FLAG as control. A 2,500-bp fragment upstream from the start codon of *OsARF11* was fused to LUC as the reporter.

(**D**) Representative of dual-luciferase reporter assay in rice protoplasts co-expressing *ProOsARF11-min35S:luc-Pro35S:Rluc* & *Pro35S:IBH1-GFP* or *ProOsARF11-min35S:luc-Pro35S:Rluc* & *Pro35S:IBH1-GFP* & *Pro35S:BU1-FLAG* or *ProOsARF11-min35S:luc-Pro35S:Rluc* & *Pro35S:IBH1-GFP* & *Pro35S:ILI1-FLAG* or *ProOsARF11-min35S:luc-Pro35S:Rluc* & *Pro35S:IBH1-GFP* & *Pro35S:ILI1-FLAG* & *Pro35S:BU1-FLAG*. Co-expressing of *ProOsARF11-min35S:luc-Pro35S:Rluc* & *Pro35S:FLAG* & *Pro35S:GFP* is used as the control (Mock). Renilla luciferase (REN) is used as an internal control. The ratio of LUC/REN represents the relative activity of promoters. ns indicates no significance. Data = means ± SD (n = 3,). The different letters above the histogram indicate significant differences (p < 0.05) by Tukey's multiple

comparison test.

(**E**) An EMSA shows that BU1 and ILI1 relieve the binding ability of IBH1 to the OsARF11 promoter. GST protein, the negative control. The plus (+) and minus (-) signs denote the presence or absence of the protein and DNA probe in each sample.

(**F**) Relative expression level of *OsARF11* in the shoot from Kitaake, *ibh1-1* and *ibh1-2* mutants at seedling stage. Asterisks indicate significant difference compared with Kitaake. Data = means ± SD (n = 3, **P < 0.01, Student's *t*-test).

(**G**) Relative expression level of *OsARF11* in the lamina joint from Kitaake, *bu1, ili1,* single mutants and *bu1/ili1* double mutants at seedling stage. Asterisks indicate significant difference compared with Kitaake. Data = means ± SD (n = 3, **P < 0.01, Student's *t*-test).

(**H**) Subcellular localization of the BU1-GFP&free FLAG and BU1-GFP&ILI1-FLAG in the leaf epidermal cells of *N. benthamiana*. D53-mCherry, a nuclear marker. Bar = 50 μm.

(**I**) The nuclear and cytoplasmic distribution of BU1-GFP protein co-expressed with FLAG or ILI1-FLAG in *N. benthamiana* leaves. Histone 3 and Actin were used as the nuclear and cytoplasm markers, respectively. C, cytoplasmic fraction; N, nuclear fraction.

(**J**) Subcellular localization of the BU1-GFP & ILI1-FLAG and BU1-GFP & FLAG in Kitaake protoplasts. SLG-mCherry, a nuclear and cytoplasm marker. Bar = 10 μm.

(**K**) and (**L**) Percentage of BU1-GFP fluorescence signal intensity in nuclear and cytoplasm. (**K**) BU1-GFP co-expressed with FLAG in Kitaake protoplasts. (**L**) BU1-GFP co-expressed with ILI1-FLAG in Kitaake protoplasts. Data = means ± SD (n = 30).

Figure 9. A proposed working model for the activation of BR responses by DEP1-mediated signaling pathways.

As BR levels increase in the plant, the nuclear localization of DEP1 is enhanced with the help of GNA. In the nucleus, DEP1, GNA and OsMYB86 likely form a complex to enhance OsMYB86's transcriptional activation of *BU1*. At the same time, BRs also upregulate the expression of *ILI1* while suppressing *IBH1* expression. The ILI1 protein then interacts with BU1, promoting its nuclear import, where both synergistically relieve the IBH1-mediated repression of *OsARF11* transcription, ultimately activating BR responses and increasing leaf inclination.

References

Bai, M.Y., Zhang, L.Y., Gampala, S.S., Zhu, S.W., Song, W.Y., Chong, K., and Wang, Z.Y. (2007). Functions of OsBZR1 and 14-3-3 proteins in brassinosteroid signaling in rice. Proc Natl Acad Sci U S A **104,** 13839-13844.

Bian, H., Xie, Y., Guo, F., Han, N., Ma, S., Zeng, Z., Wang, J., Yang, Y., and Zhu, M. (2012). Distinctive expression patterns and roles of the miRNA393/TIR1 homolog module in regulating flag leaf inclination and primary and crown root growth in rice (Oryza sativa). New Phytol **196,** 149-161.

Bishop, G.J., and Koncz, C. (2002). Brassinosteroids and plant steroid hormone signaling. Plant Cell **14 Suppl,** S97-

110.

Che, R., Tong, H., Shi, B., Liu, Y., Fang, S., Liu, D., Xiao, Y., Hu, B., Liu, L., Wang, H., Zhao, M., and Chu, C. (2015). Control of grain size and rice yield by GL2-mediated brassinosteroid responses. Nat Plants **2,** 15195.

Chen, H., Yu, H., Jiang, W., Li, H., Wu, T., Chu, J., Xin, P., Li, Z., Wang, R., Zhou, T., Huang, K., Lu, L., Bian, M., and Du, X. (2021). Overexpression of ovate family protein 22 confers multiple morphological changes and represses gibberellin and brassinosteroid signalings in transgenic rice. Plant Sci **304,** 110734.

Chen, L., Xiong, G., Cui, X., Yan, M., Xu, T., Qian, Q., Xue, Y., Li, J., and Wang, Y. (2013). OsGRAS19 may be a novel component involved in the brassinosteroid signaling pathway in rice. Mol Plant **6,** 988-991.

Clouse, S.D. (2011). Brassinosteroid signal transduction: from receptor kinase activation to transcriptional networks regulating plant development. Plant Cell **23,** 1219-1230.

Dastidar, M.G., Scarpa, A., Magele, I., Ruiz-Duarte, P., von Born, P., Bald, L., Jouannet, V., and Maizel, A. (2019). ARF5/MONOPTEROS directly regulates miR390 expression in the Arabidopsis thaliana primary root meristem. Plant Direct **3,** e00116.

Duan, P., Ni, S., Wang, J., Zhang, B., Xu, R., Wang, Y., Chen, H., Zhu, X., and Li, Y. (2015). Regulation of OsGRF4 by OsmiR396 controls grain size and yield in rice. Nat Plants **2,** 15203.

Feller, A., Machemer, K., Braun, E.L., and Grotewold, E. (2011). Evolutionary and comparative analysis of MYB and bHLH plant transcription factors. Plant J **66,** 94-116.

Feng, Z., Wu, C., Wang, C., Roh, J., Zhang, L., Chen, J., Zhang, S., Zhang, H., Yang, C., Hu, J., You, X., Liu, X., Yang, X., Guo, X., Zhang, X., Wu, F., Terzaghi, W., Kim, S.K., Jiang, L., and Wan, J. (2016). SLG controls grain size and leaf angle by modulating brassinosteroid homeostasis in rice. J Exp Bot **67,** 4241-4253.

Gampala, S.S., Kim, T.W., He, J.X., Tang, W., Deng, Z., Bai, M.Y., Guan, S., Lalonde, S., Sun, Y., Gendron, J.M., Chen, H., Shibagaki, N., Ferl, R.J., Ehrhardt, D., Chong, K., Burlingame, A.L., and Wang, Z.Y. (2007). An essential role for 14-3-3 proteins in brassinosteroid signal transduction in Arabidopsis. Dev Cell **13,** 177-189.

Gao, J., Chen, H., Yang, H., He, Y., Tian, Z., and Li, J. (2018). A brassinosteroid responsive miRNA-target module regulates gibberellin biosynthesis and plant development. New Phytol **220,** 488-501.

Gilman, A.G. (1987). G proteins: transducers of receptor-generated signals. Annu Rev Biochem **56,** 615-649.

Guo, J., Li, W., Shang, L., Wang, Y., Yan, P., Bai, Y., Da, X., Wang, K., Guo, Q., Jiang, R., Mao, C., and Mo, X. (2021). OsbHLH98 regulates leaf angle in rice through transcriptional repression of OsBUL1. New Phytol **230,** 1953-1966.

Guo, M., Zhang, Y., Jia, X., Wang, X., Zhang, Y., Liu, J., Yang, Q., Ruan, W., and Yi, K. (2022). Alternative splicing of REGULATOR OF LEAF INCLINATION 1 modulates phosphate starvation signaling and growth in plants. Plant Cell **34,** 3319-3338.

Hao, Y., Zong, X., Ren, P., Qian, Y., and Fu, A. (2021). Basic Helix-Loop-Helix (bHLH) Transcription Factors Regulate a Wide Range of Functions in Arabidopsis. Int J Mol Sci **22**.

He, J.X., Gendron, J.M., Sun, Y., Gampala, S.S., Gendron, N., Sun, C.Q., and Wang, Z.Y. (2005). BZR1 is a transcriptional repressor with dual roles in brassinosteroid homeostasis and growth responses. Science **307,** 1634-1638.

Hirsch, S., Kim, J., Munoz, A., Heckmann, A.B., Downie, J.A., and Oldroyd, G.E. (2009). GRAS proteins form a DNA binding complex to induce gene expression during nodulation signaling in Medicago truncatula. Plant Cell **21,** 545-557.

Hong, Z., Ueguchi-Tanaka, M., Fujioka, S., Takatsuto, S., Yoshida, S., Hasegawa, Y., Ashikari, M., Kitano, H., and Matsuoka, M. (2005). The Rice brassinosteroid-deficient dwarf2 mutant, defective in the rice homolog of Arabidopsis DIMINUTO/DWARF1, is rescued by the endogenously accumulated alternative bioactive brassinosteroid, dolichosterone. Plant Cell **17,** 2243-2254.

Hong, Z., Ueguchi-Tanaka, M., Umemura, K., Uozu, S., Fujioka, S., Takatsuto, S., Yoshida, S., Ashikari, M., Kitano, H., and Matsuoka, M. (2003). A rice brassinosteroid-deficient mutant, ebisu dwarf (d2), is caused by a loss of function of a new member of cytochrome P450. Plant Cell **15,** 2900-2910.

Hothorn, M., Belkhadir, Y., Dreux, M., Dabi, T., Noel, J.P., Wilson, I.A., and Chory, J. (2011). Structural basis of steroid hormone perception by the receptor kinase BRI1. Nature **474,** 467-471.

Hu, X., Qian, Q., Xu, T., Zhang, Y., Dong, G., Gao, T., Xie, Q., and Xue, Y. (2013). The U-box E3 ubiquitin ligase TUD1 functions with a heterotrimeric G alpha subunit to regulate Brassinosteroid-mediated growth in rice. PLoS Genet **9,** e1003391.

Huang, G., Hu, H., van de Meene, A., Zhang, J., Dong, L., Zheng, S., Zhang, F., Betts, N.S., Liang, W., Bennett, M.J., Persson, S., and Zhang, D. (2021). AUXIN RESPONSE FACTORS 6 and 17 control the flag leaf angle in rice by regulating secondary cell wall biosynthesis of lamina joints. Plant Cell **33,** 3120-3133.

Huang, X., Qian, Q., Liu, Z., Sun, H., He, S., Luo, D., Xia, G., Chu, C., Li, J., and Fu, X. (2009). Natural variation at the DEP1 locus enhances grain yield in rice. Nat Genet **41,** 494-497.

Jang, S., An, G., and Li, H.Y. (2017). Rice Leaf Angle and Grain Size Are Affected by the OsBUL1 Transcriptional Activator Complex. Plant Physiol **173,** 688-702.

Kim, E.J., and Russinova, E. (2020). Brassinosteroid signalling. Curr Biol **30,** R294-R298.

Kim, T.W., Guan, S., Burlingame, A.L., and Wang, Z.Y. (2011). The CDG1 kinase mediates brassinosteroid signal transduction from BRI1 receptor kinase to BSU1 phosphatase and GSK3-like kinase BIN2. Mol Cell **43,** 561-571.

Li, J., and Nam, K.H. (2002). Regulation of brassinosteroid signaling by a GSK3/SHAGGY-like kinase. Science **295,** 1299-1301.

Li, Q., Xu, F., Chen, Z., Teng, Z., Sun, K., Li, X., Yu, J., Zhang, G., Liang, Y., Huang, X., Du, L., Qian, Y., Wang, Y., Chu, C., and Tang, J. (2021). Synergistic interplay of ABA and BR signal in regulating plant growth and adaptation. Nat Plants **7,** 1108-1118.

Li, Q.F., Lu, J., Zhou, Y., Wu, F., Tong, H.N., Wang, J.D., Yu, J.W., Zhang, C.Q., Fan, X.L., and Liu, Q.Q. (2019). Abscisic Acid Represses Rice Lamina Joint Inclination by Antagonizing Brassinosteroid Biosynthesis and Signaling. Int J Mol Sci **20**.

Liu, D., Zhang, X., Li, Q., Xiao, Y., Zhang, G., Yin, W., Niu, M., Meng, W., Dong, N., Liu, J., Yang, Y., Xie, Q., Chu, C., and Tong, H. (2023). The U-box ubiquitin ligase TUD1 promotes brassinosteroid-induced GSK2 degradation in rice. Plant Commun **4,** 100450.

Liu, Q., Han, R., Wu, K., Zhang, J., Ye, Y., Wang, S., Chen, J., Pan, Y., Li, Q., Xu, X., Zhou, J., Tao, D., Wu, Y., and Fu, X. (2018). G-protein betagamma subunits determine grain size through interaction with MADS-

domain transcription factors in rice. Nat Commun **9,** 852.

Matsuta, S., Nishiyama, A., Chaya, G., Itoh, T., Miura, K., and Iwasaki, Y. (2018). Characterization of Heterotrimeric G Protein gamma4 Subunit in Rice. Int J Mol Sci **19**.

Miao, J., Guo, D., Zhang, J., Huang, Q., Qin, G., Zhang, X., Wan, J., Gu, H., and Qu, L.J. (2013). Targeted mutagenesis in rice using CRISPR-Cas system. Cell Res **23,** 1233-1236.

Miao Liu, J., Mei, Q., Yun Xue, C., Yuan Wang, Z., Pin Li, D., Xin Zhang, Y., and Hu Xuan, Y. (2021). Mutation of G-protein gamma subunit DEP1 increases planting density and resistance to sheath blight disease in rice. Plant Biotechnol J **19,** 418-420.

Millard, P.S., Kragelund, B.B., and Burow, M. (2019). R2R3 MYB Transcription Factors - Functions outside the DNA-Binding Domain. Trends Plant Sci **24,** 934-946.

Mori, M., Nomura, T., Ooka, H., Ishizaka, M., Yokota, T., Sugimoto, K., Okabe, K., Kajiwara, H., Satoh, K., Yamamoto, K., Hirochika, H., and Kikuchi, S. (2002). Isolation and characterization of a rice dwarf mutant with a defect in brassinosteroid biosynthesis. Plant Physiol **130,** 1152-1161.

Morita, M.T., and Tasaka, M. (2004). Gravity sensing and signaling. Curr Opin Plant Biol **7,** 712-718.

Nakashita, H., Yasuda, M., Nitta, T., Asami, T., Fujioka, S., Arai, Y., Sekimata, K., Takatsuto, S., Yamaguchi, I., and Yoshida, S. (2003). Brassinosteroid functions in a broad range of disease resistance in tobacco and rice. Plant J **33,** 887-898.

Ning, J., Zhang, B., Wang, N., Zhou, Y., and Xiong, L. (2011). Increased leaf angle1, a Raf-like MAPKKK that interacts with a nuclear protein family, regulates mechanical tissue formation in the Lamina joint of rice. Plant Cell **23,** 4334-4347.

Nolan, T.M., Vukasinovic, N., Liu, D., Russinova, E., and Yin, Y. (2020). Brassinosteroids: Multidimensional Regulators of Plant Growth, Development, and Stress Responses. Plant Cell **32,** 295-318.

Park, H.S., Ryu, H.Y., Kim, B.H., Kim, S.Y., Yoon, I.S., and Nam, K.H. (2011). A subset of OsSERK genes, including OsBAK1, affects normal growth and leaf development of rice. Mol Cells **32,** 561-569.

Qiao, J., Zhang, Y., Han, S., Chang, S., Gao, Z., Qi, Y., and Qian, Q. (2022). OsARF4 regulates leaf inclination via auxin and brassinosteroid pathways in rice. Front Plant Sci **13,** 979033.

Qiao, S., Sun, S., Wang, L., Wu, Z., Li, C., Li, X., Wang, T., Leng, L., Tian, W., Lu, T., and Wang, X. (2017). The RLA1/SMOS1 Transcription Factor Functions with OsBZR1 to Regulate Brassinosteroid Signaling and Rice Architecture. Plant Cell **29,** 292-309.

Ruan, W., Guo, M., Xu, L., Wang, X., Zhao, H., Wang, J., and Yi, K. (2018). An SPX-RLI1 Module Regulates Leaf Inclination in Response to Phosphate Availability in Rice. Plant Cell **30,** 853-870.

Sakamoto, T., Morinaka, Y., Inukai, Y., Kitano, H., and Fujioka, S. (2013). Auxin signal transcription factor regulates expression of the brassinosteroid receptor gene in rice. Plant J **73,** 676-688.

Sakamoto, T., Morinaka, Y., Ohnishi, T., Sunohara, H., Fujioka, S., Ueguchi-Tanaka, M., Mizutani, M., Sakata, K., Takatsuto, S., Yoshida, S., Tanaka, H., Kitano, H., and Matsuoka, M. (2006). Erect leaves caused by brassinosteroid deficiency increase biomass production and grain yield in rice. Nat Biotechnol **24,** 105-109.

Shimada, A., Ueguchi-Tanaka, M., Sakamoto, T., Fujioka, S., Takatsuto, S., Yoshida, S., Sazuka, T., Ashikari, M., and Matsuoka, M. (2006). The rice SPINDLY gene functions as a negative regulator of gibberellin signaling by controlling the suppressive function of the DELLA protein, SLR1, and modulating

brassinosteroid synthesis. Plant J **48,** 390-402.

Sims, K., Abedi-Samakush, F., Szulc, N., Macias Honti, M.G., and Mattsson, J. (2021). OsARF11 Promotes Growth, Meristem, Seed, and Vein Formation during Rice Plant Development. Int J Mol Sci **22**.

Song, Y., You, J., and Xiong, L. (2009). Characterization of OsIAA1 gene, a member of rice Aux/IAA family involved in auxin and brassinosteroid hormone responses and plant morphogenesis. Plant Mol Biol **70,** 297-309.

Sun, H., Qian, Q., Wu, K., Luo, J., Wang, S., Zhang, C., Ma, Y., Liu, Q., Huang, X., Yuan, Q., Han, R., Zhao, M., Dong, G., Guo, L., Zhu, X., Gou, Z., Wang, W., Wu, Y., Lin, H., and Fu, X. (2014). Heterotrimeric G proteins regulate nitrogen-use efficiency in rice. Nat Genet **46,** 652-656.

Sun, S., Chen, D., Li, X., Qiao, S., Shi, C., Li, C., Shen, H., and Wang, X. (2015). Brassinosteroid signaling regulates leaf erectness in Oryza sativa via the control of a specific U-type cyclin and cell proliferation. Dev Cell **34,** 220-228.

Sun, S., Wang, L., Mao, H., Shao, L., Li, X., Xiao, J., Ouyang, Y., and Zhang, Q. (2018). A G-protein pathway determines grain size in rice. Nat Commun **9,** 851.

Sun, Y., Fan, X.Y., Cao, D.M., Tang, W., He, K., Zhu, J.Y., He, J.X., Bai, M.Y., Zhu, S., Oh, E., Patil, S., Kim, T.W., Ji, H., Wong, W.H., Rhee, S.Y., and Wang, Z.Y. (2010). Integration of brassinosteroid signal transduction with the transcription network for plant growth regulation in Arabidopsis. Dev Cell **19,** 765-777.

Taguchi-Shiobara, F., Kawagoe, Y., Kato, H., Onodera, H., Tagiri, A., Hara, N., Miyao, A., Hirochika, H., Kitano, H., Yano, M., and Toki, S. (2011). A loss-of-function mutation of rice causes semi-dwarfness and slightly increased number of spikelets. Breeding Sci **61,** 17-25.

Tanabe, S., Ashikari, M., Fujioka, S., Takatsuto, S., Yoshida, S., Yano, M., Yoshimura, A., Kitano, H., Matsuoka, M., Fujisawa, Y., Kato, H., and Iwasaki, Y. (2005). A novel cytochrome P450 is implicated in brassinosteroid biosynthesis via the characterization of a rice dwarf mutant, dwarf11, with reduced seed length. Plant Cell **17,** 776-790.

Tanaka, A., Nakagawa, H., Tomita, C., Shimatani, Z., Ohtake, M., Nomura, T., Jiang, C.J., Dubouzet, J.G., Kikuchi, S., Sekimoto, H., Yokota, T., Asami, T., Kamakura, T., and Mori, M. (2009). BRASSINOSTEROID UPREGULATED1, encoding a helix-loop-helix protein, is a novel gene involved in brassinosteroid signaling and controls bending of the lamina joint in rice. Plant Physiol **151,** 669-680.

Tang, W., Kim, T.W., Oses-Prieto, J.A., Sun, Y., Deng, Z., Zhu, S., Wang, R., Burlingame, A.L., and Wang, Z.Y. (2008). BSKs mediate signal transduction from the receptor kinase BRI1 in Arabidopsis. Science **321,** 557-560.

Teng, S., Liu, Q., Chen, G., Chang, Y., Cui, X., Wu, J., Ai, P., Sun, X., Zhang, Z., and Lu, T. (2023). OsbHLH92, in the noncanonical brassinosteroid signaling pathway, positively regulates leaf angle and grain weight in rice. New Phytol **240,** 1066-1081.

Tong, H., and Chu, C. (2017). Physiological Analysis of Brassinosteroid Responses and Sensitivity in Rice. Methods Mol Biol **1564,** 23-29.

Tong, H., and Chu, C. (2018). Functional Specificities of Brassinosteroid and Potential Utilization for Crop Improvement. Trends Plant Sci **23,** 1016-1028.

Tong, H., Liu, L., Jin, Y., Du, L., Yin, Y., Qian, Q., Zhu, L., and Chu, C. (2012). DWARF AND LOW-TILLERING acts as a direct downstream target of a GSK3/SHAGGY-like kinase to mediate brassinosteroid responses in

rice. Plant Cell **24,** 2562-2577.

Tong, H., Jin, Y., Liu, W., Li, F., Fang, J., Yin, Y., Qian, Q., Zhu, L., and Chu, C. (2009). DWARF AND LOW-TILLERING, a new member of the GRAS family, plays positive roles in brassinosteroid signaling in rice. Plant J **58,** 803-816.

Ueguchi-Tanaka, M., Fujisawa, Y., Kobayashi, M., Ashikari, M., Iwasaki, Y., Kitano, H., and Matsuoka, M. (2000). Rice dwarf mutant d1, which is defective in the alpha subunit of the heterotrimeric G protein, affects gibberellin signal transduction. Proc Natl Acad Sci U S A **97,** 11638-11643.

Urano, D., and Jones, A.M. (2014). Heterotrimeric G protein-coupled signaling in plants. Annu Rev Plant Biol **65,** 365-384.

Urano, D., Chen, J.G., Botella, J.R., and Jones, A.M. (2013). Heterotrimeric G protein signalling in the plant kingdom. Open Biol **3,** 120186.

Waadt, R., and Kudla, J. (2008). In Planta Visualization of Protein Interactions Using Bimolecular Fluorescence Complementation (BiFC). CSH Protoc **2008,** pdb prot4995.

Wang, L., Xu, Y.Y., Ma, Q.B., Li, D., Xu, Z.H., and Chong, K. (2006). Heterotrimeric G protein alpha subunit is involved in rice brassinosteroid response. Cell Res **16,** 916-922.

Wang, Q.L., Sun, A.Z., Chen, S.T., Chen, L.S., and Guo, F.Q. (2018). SPL6 represses signalling outputs of ER stress in control of panicle cell death in rice. Nat Plants **4,** 280-288.

Wang, X., and Chory, J. (2006). Brassinosteroids regulate dissociation of BKI1, a negative regulator of BRI1 signaling, from the plasma membrane. Science **313,** 1118-1122.

Wang, Y., Lv, Y., Yu, H., Hu, P., Wen, Y., Wang, J., Tan, Y., Wu, H., Zhu, L., Wu, K., Chai, B., Liu, J., Zeng, D., Zhang, G., Zhu, L., Gao, Z., Dong, G., Ren, D., Shen, L., Zhang, Q., Li, Q., Guo, L., Xiong, G., Qian, Q., and Hu, J. (2024). GR5 acts in the G protein pathway to regulate grain size in rice. Plant Commun **5,** 100673.

Xiao, Y., Liu, D., Zhang, G., Tong, H., and Chu, C. (2017). Brassinosteroids Regulate OFP1, a DLT Interacting Protein, to Modulate Plant Architecture and Grain Morphology in Rice. Front Plant Sci **8,** 1698.

Yamamuro, C., Ihara, Y., Wu, X., Noguchi, T., Fujioka, S., Takatsuto, S., Ashikari, M., Kitano, H., and Matsuoka, M. (2000). Loss of function of a rice brassinosteroid insensitive1 homolog prevents internode elongation and bending of the lamina joint. Plant Cell **12,** 1591-1606.

Yanhui, C., Xiaoyuan, Y., Kun, H., Meihua, L., Jigang, L., Zhaofeng, G., Zhiqiang, L., Yunfei, Z., Xiaoxiao, W., Xiaoming, Q., Yunping, S., Li, Z., Xiaohui, D., Jingchu, L., Xing-Wang, D., Zhangliang, C., Hongya, G., and Li-Jia, Q. (2006). The MYB transcription factor superfamily of Arabidopsis: expression analysis and phylogenetic comparison with the rice MYB family. Plant Mol Biol **60,** 107-124.

Zhang, C., Xu, Y., Guo, S., Zhu, J., Huan, Q., Liu, H., Wang, L., Luo, G., Wang, X., and Chong, K. (2012). Dynamics of brassinosteroid response modulated by negative regulator LIC in rice. PLoS Genet **8,** e1002686.

Zhang, D.P., Zhou, Y., Yin, J.F., Yan, X.J., Lin, S., Xu, W.F., Baluska, F., Wang, Y.P., Xia, Y.J., Liang, G.H., and Liang, J.S. (2015a). Rice G-protein subunits qPE9-1 and RGB1 play distinct roles in abscisic acid responses and drought adaptation. J Exp Bot **66,** 6371-6384.

Zhang, J., Lin, Q., Wang, X., Shao, J., Ren, Y., Liu, X., Feng, M., Li, S., Sun, Q., Luo, S., Liu, B., Xing, X., Chang, Y., Cheng, Z., and Wan, J. (2024). The DENSE AND ERECT PANICLE1-GRAIN NUMBER

ASSOCIATED module enhances rice yield by repressing CYTOKININ OXIDASE 2 expression. Plant Cell **37**.

Zhang, L.Y., Bai, M.Y., Wu, J., Zhu, J.Y., Wang, H., Zhang, Z., Wang, W., Sun, Y., Zhao, J., Sun, X., Yang, H., Xu, Y., Kim, S.H., Fujioka, S., Lin, W.H., Chong, K., Lu, T., and Wang, Z.Y. (2009a). Antagonistic HLH/bHLH transcription factors mediate brassinosteroid regulation of cell elongation and plant development in rice and Arabidopsis. Plant Cell **21,** 3767-3780.

Zhang, S., Wang, S., Xu, Y., Yu, C., Shen, C., Qian, Q., Geisler, M., Jiang de, A., and Qi, Y. (2015b). The auxin response factor, OsARF19, controls rice leaf angles through positively regulating OsGH3-5 and OsBRI1. Plant Cell Environ **38,** 638-654.

Zhang, S.W., Li, C.H., Cao, J., Zhang, Y.C., Zhang, S.Q., Xia, Y.F., Sun, D.Y., and Sun, Y. (2009b). Altered architecture and enhanced drought tolerance in rice via the down-regulation of indole-3-acetic acid by TLD1/OsGH3.13 activation. Plant Physiol **151,** 1889-1901.

Zhang, Y., Su, J., Duan, S., Ao, Y., Dai, J., Liu, J., Wang, P., Li, Y., Liu, B., Feng, D., Wang, J., and Wang, H. (2011). A highly efficient rice green tissue protoplast system for transient gene expression and studying light/chloroplast-related processes. Plant Methods **7,** 30.

Zhao, B., and Li, J. (2012). Regulation of brassinosteroid biosynthesis and inactivation. J Integr Plant Biol **54,** 746-759.

Zhou, F., Lin, Q., Zhu, L., Ren, Y., Zhou, K., Shabek, N., Wu, F., Mao, H., Dong, W., Gan, L., Ma, W., Gao, H., Chen, J., Yang, C., Wang, D., Tan, J., Zhang, X., Guo, X., Wang, J., Jiang, L., Liu, X., Chen, W., Chu, J., Yan, C., Ueno, K., Ito, S., Asami, T., Cheng, Z., Wang, J., Lei, C., Zhai, H., Wu, C., Wang, H., Zheng, N., and Wan, J. (2013). D14-SCF(D3)-dependent degradation of D53 regulates strigolactone signalling. Nature **504,** 406-410.

Zhou, L.J., Xiao, L.T., and Xue, H.W. (2017). Dynamic Cytology and Transcriptional Regulation of Rice Lamina Joint Development. Plant Physiol **174,** 1728-1746.

Zhou, Y., Zhu, J., Li, Z., Yi, C., Liu, J., Zhang, H., Tang, S., Gu, M., and Liang, G. (2009). Deletion in a quantitative trait gene qPE9-1 associated with panicle erectness improves plant architecture during rice domestication. Genetics **183,** 315-324.

Zhu, C.L., Xing, B., Teng, S.Z., Deng, C., Shen, Z.Y., Ai, P.F., Lu, T.G., Zhang, S.W., and Zhang, Z.G. (2021). OsRELA Regulates Leaf Inclination by Repressing the Transcriptional Activity of OsLIC in Rice. Front Plant Sci **12,** 760041.

Zou, T., Zhang, K., Zhang, J., Liu, S., Liang, J., Liu, J., Zhu, J., Liang, Y., Wang, S., Deng, Q., Liu, H., Jin, J., Li, P., and Li, S. (2023). DWARF AND LOW-TILLERING 2 functions in brassinosteroid signaling and controls plant architecture and grain size in rice. Plant J **116,** 1766-1783.

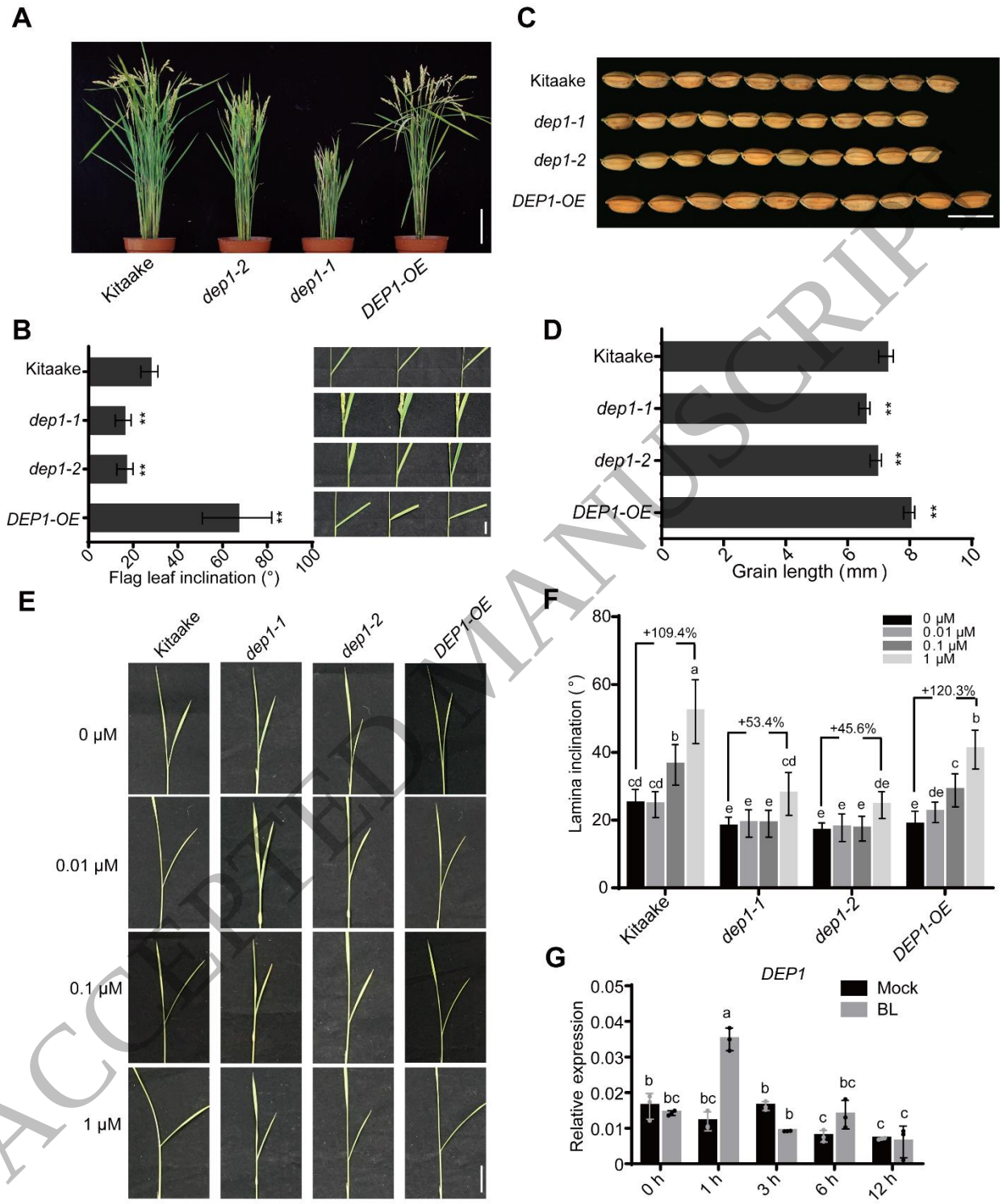

Figure 1

163x197 mm (x DPI)

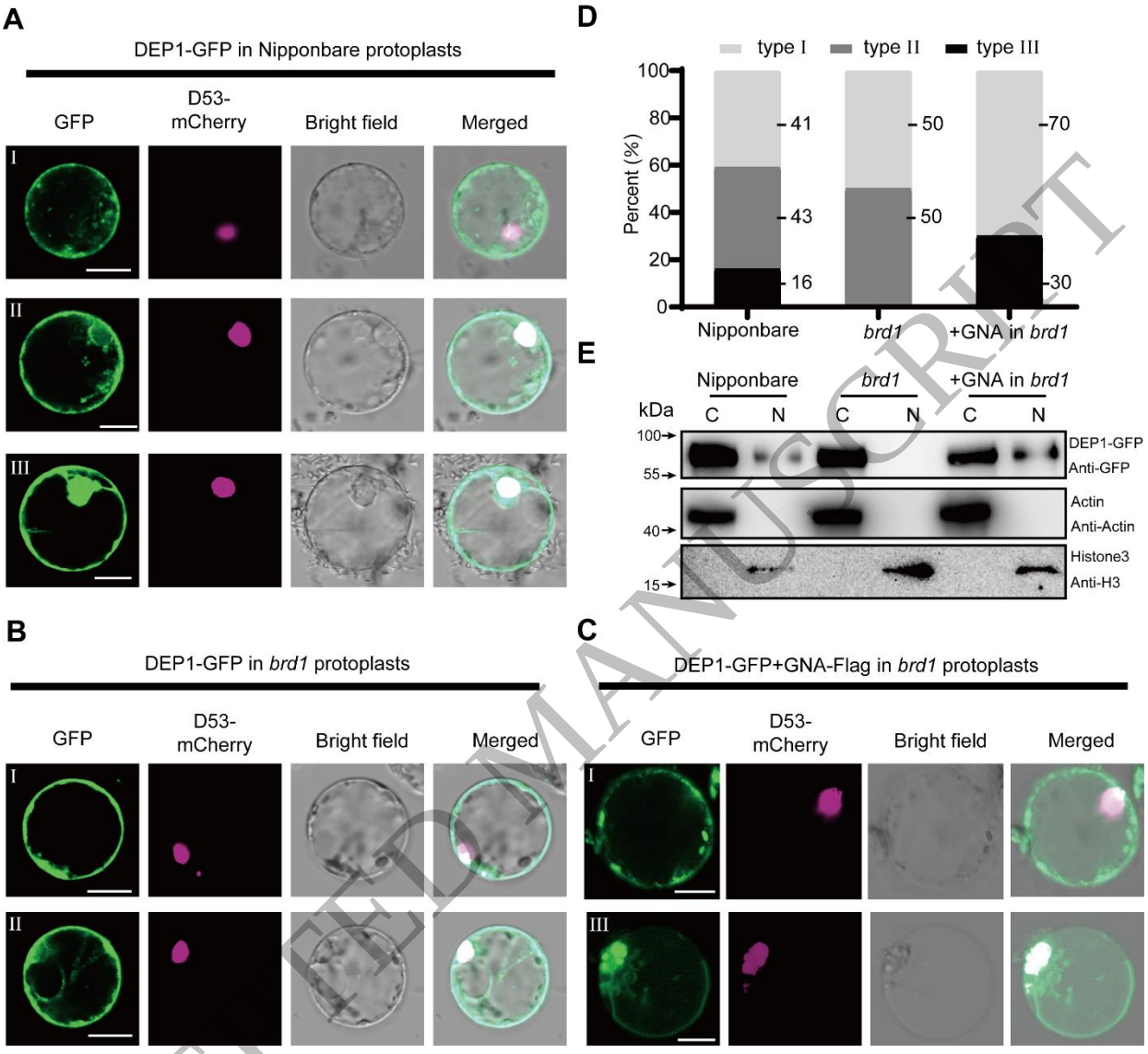

Figure 2

164x150 mm (x DPI)

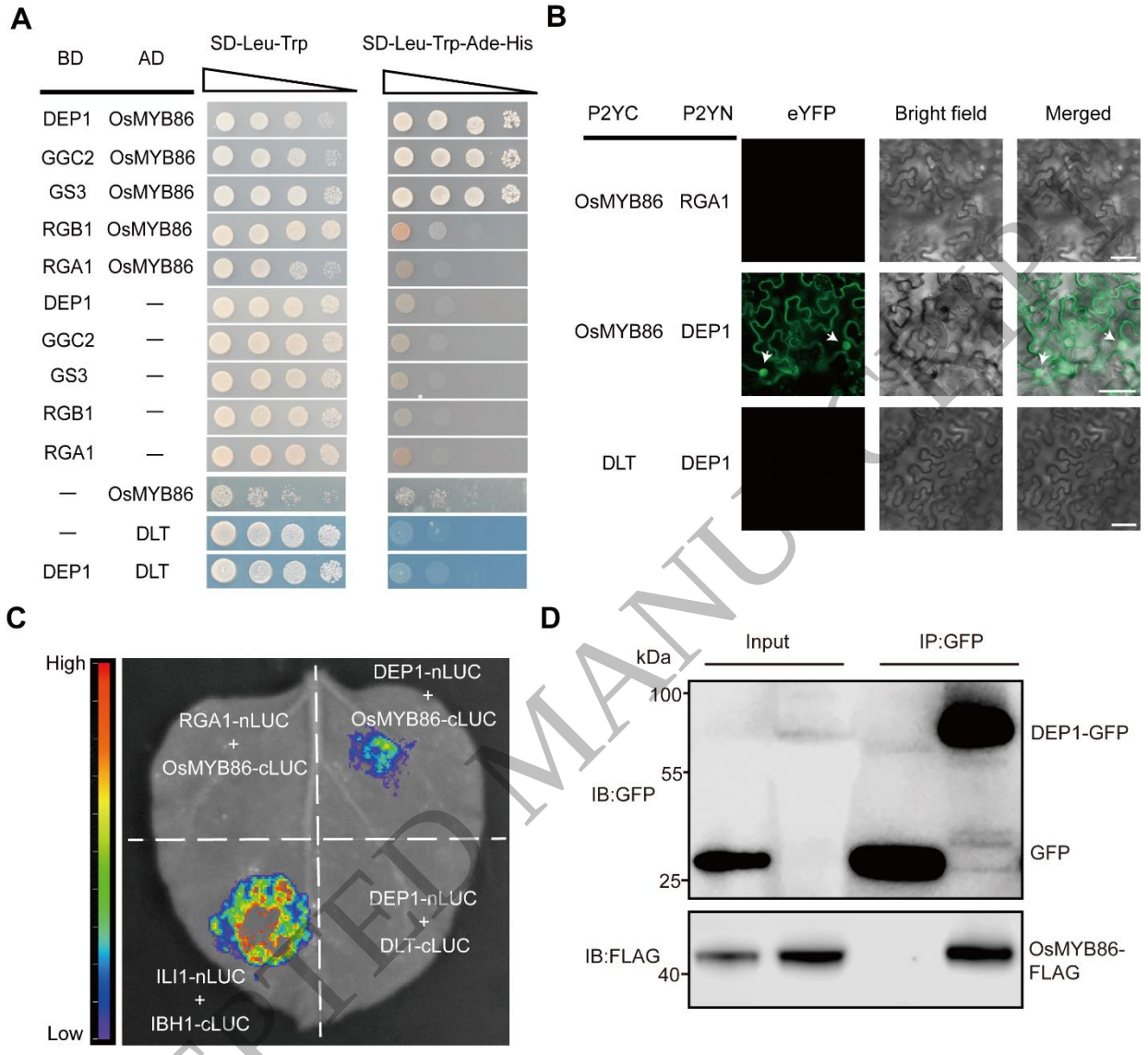

Figure 3

162x150 mm (x DPI)

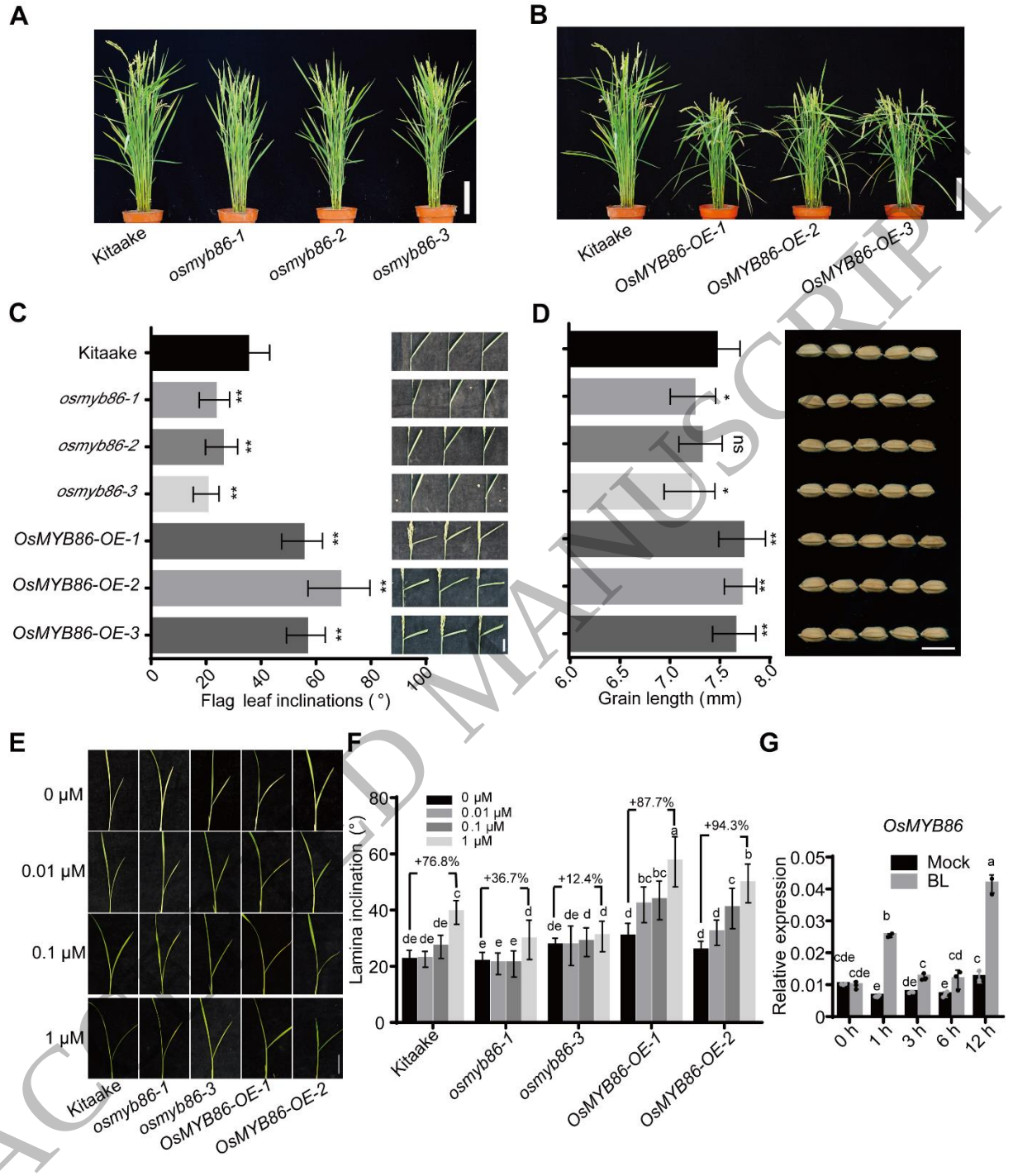

Figure 4

160x186 mm (x DPI)

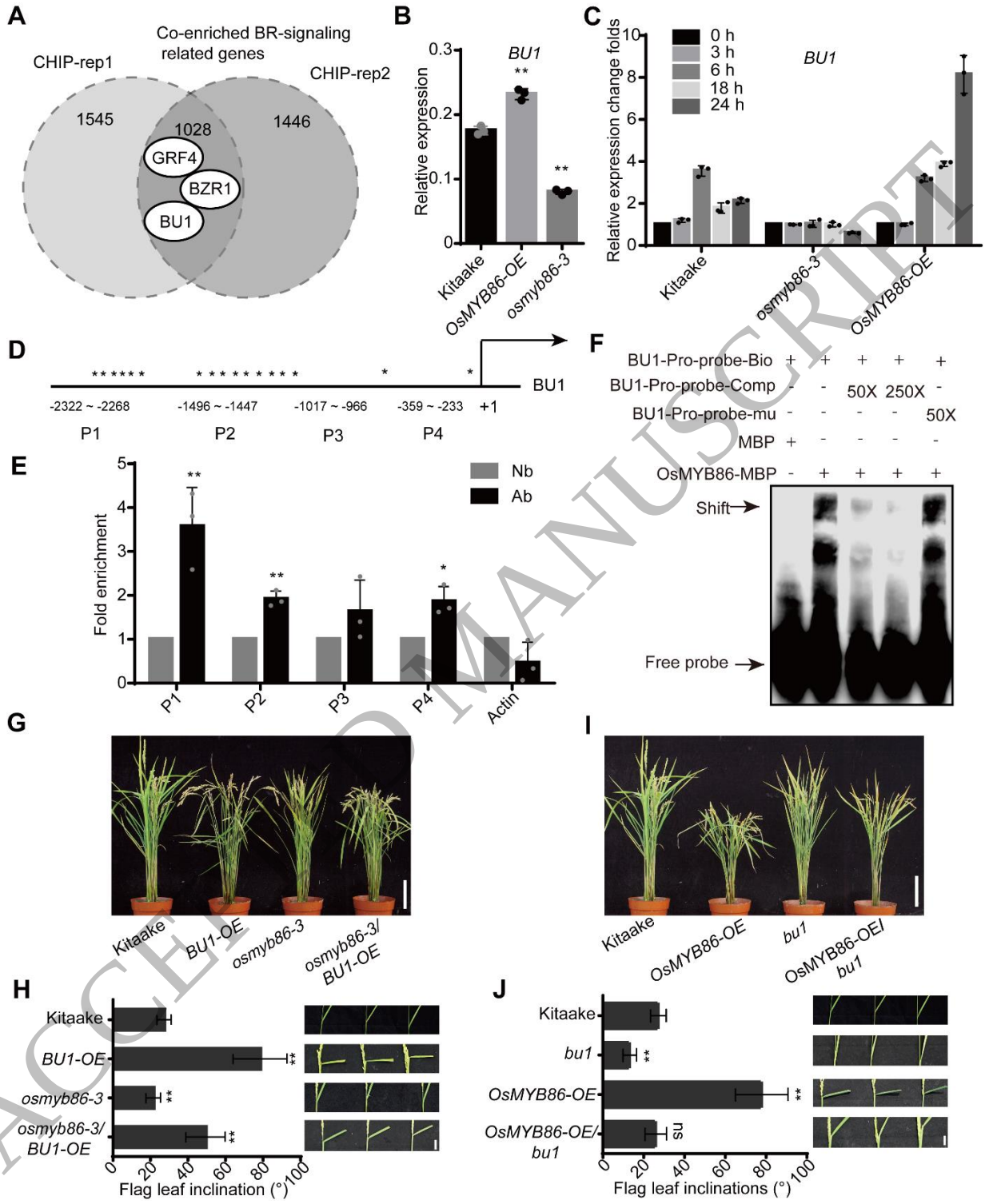

Figure 5

162x198 mm (x DPI)

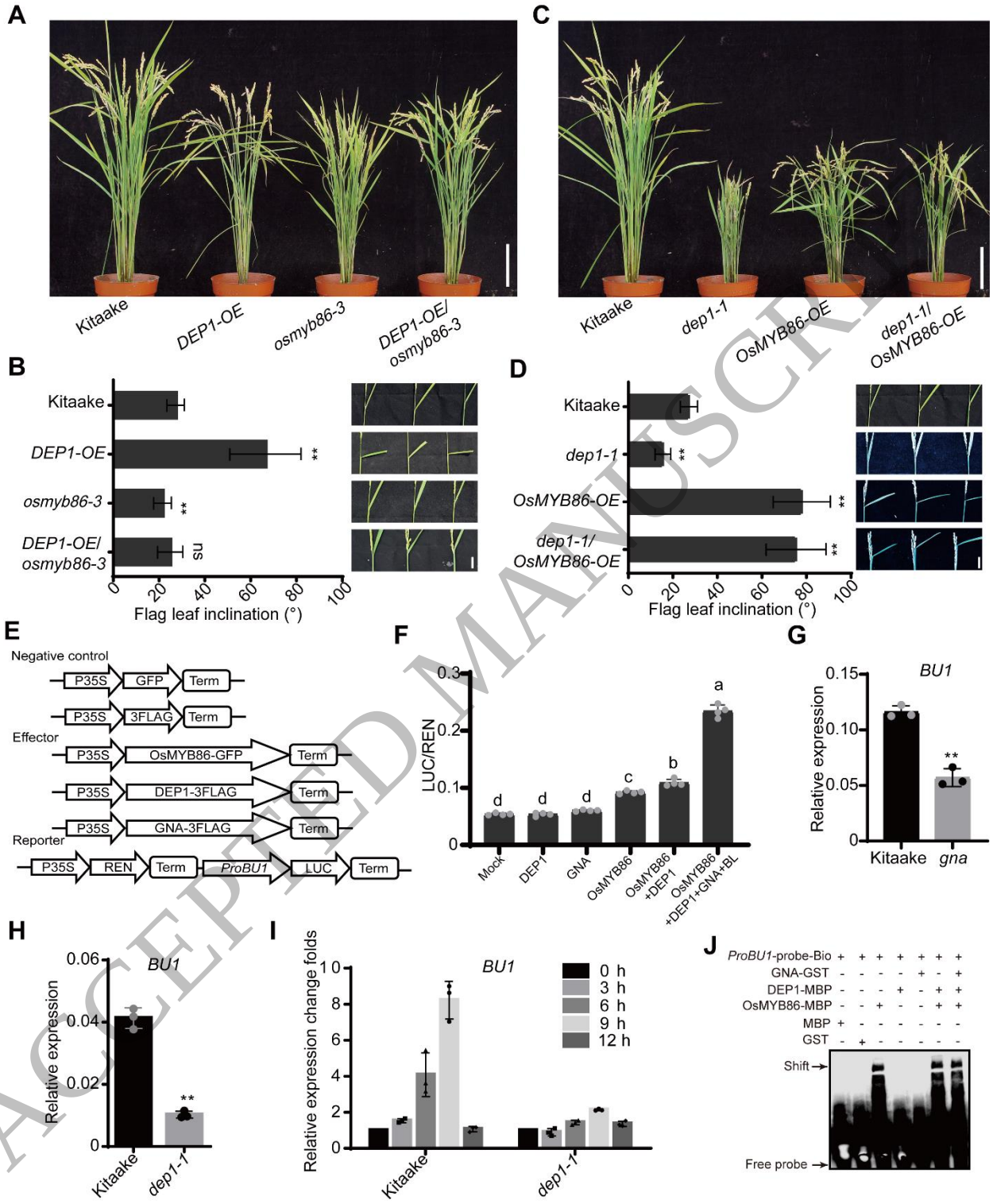

Figure 6

164x200 mm (x DPI)

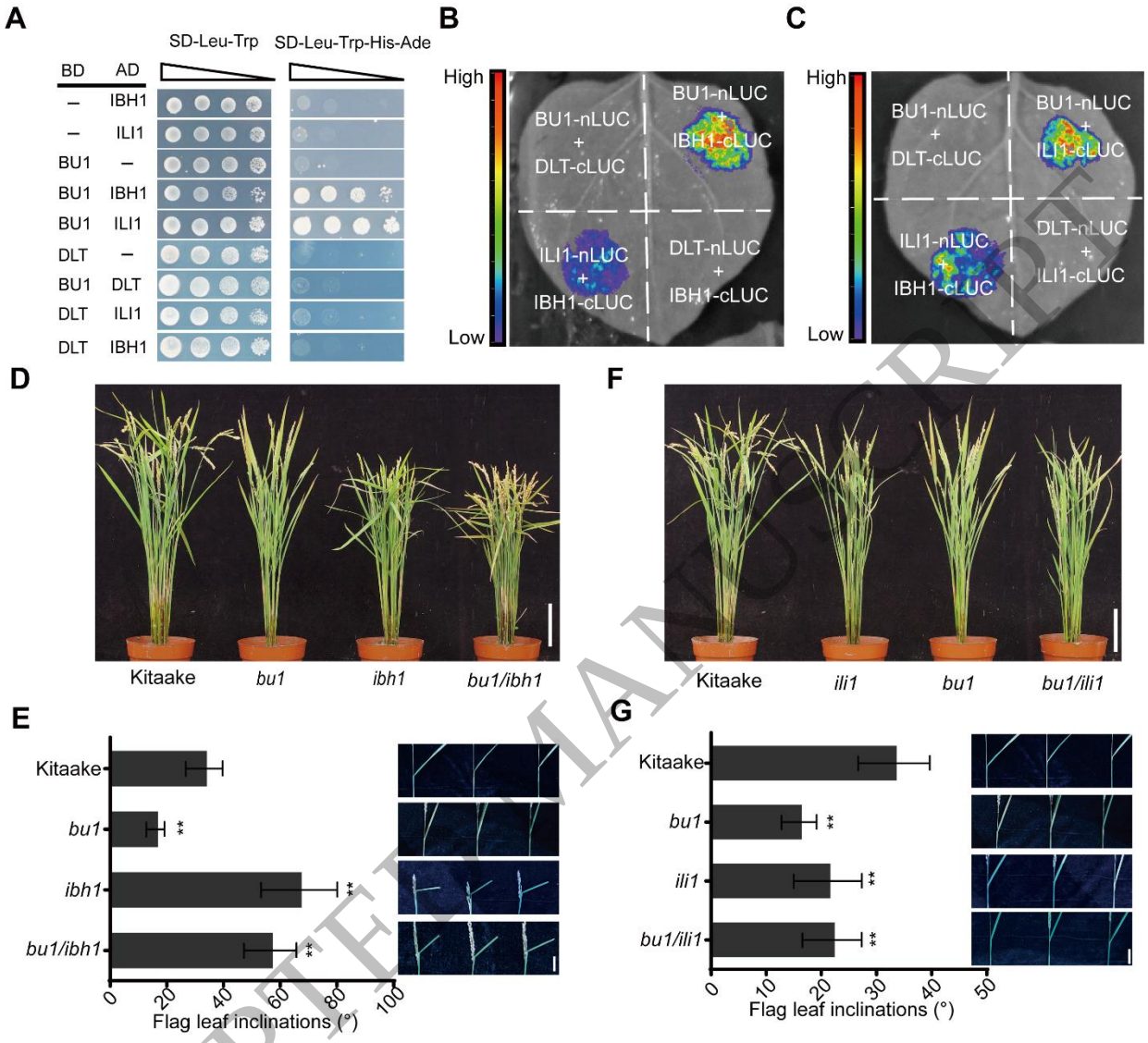

Figure 7

163x148 mm (x DPI)

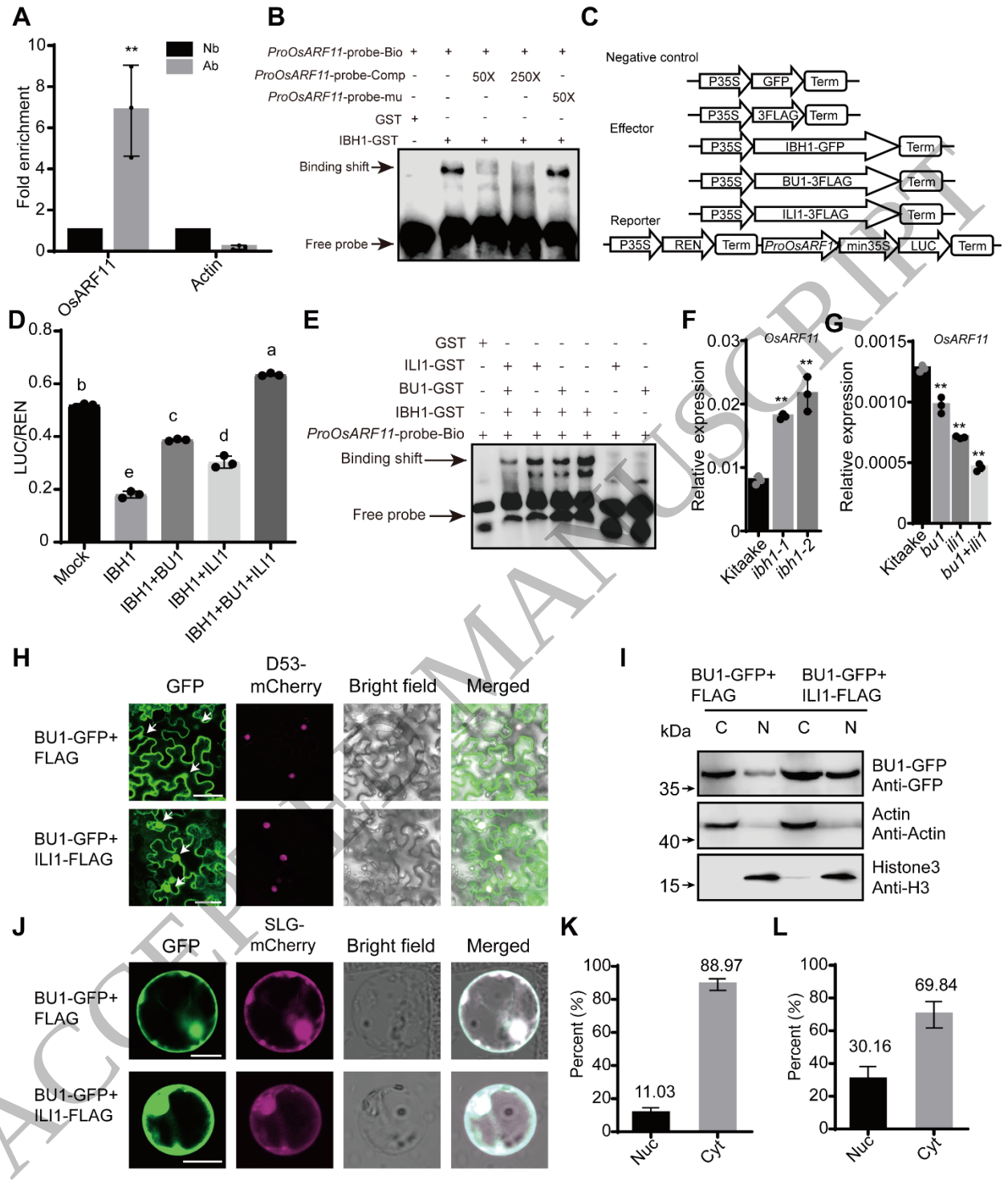

Figure 8

164x192 mm (x DPI)

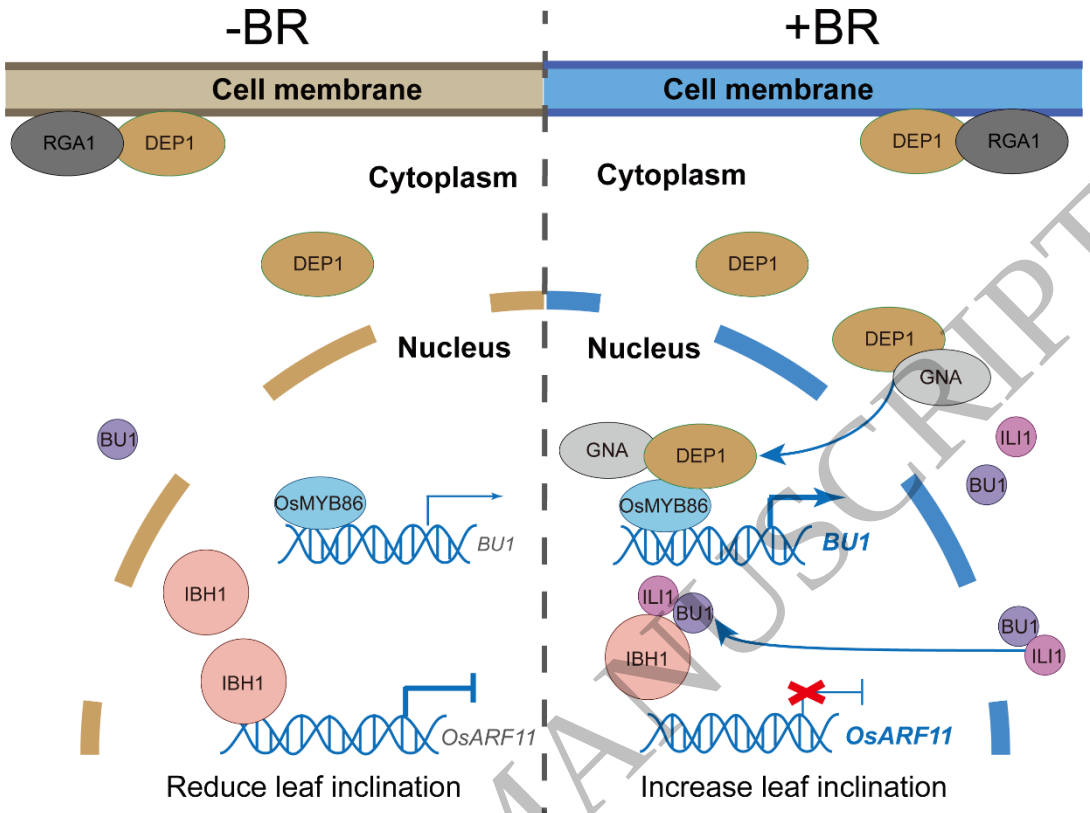

Figure 9

142x109 mm (x DPI)